

# Caudal Topographic Nucleus Isthmi and the Rostral Nontopographic Nucleus Isthmi in the Turtle, *Pseudemys scripta*

MARTIN I. SERENO AND PHILIP S. ULINSKI

Committees on Neurobiology (M.I.S., P.S.U.) and on the Conceptual Foundations of Science (M.I.S.), and Department of Anatomy (P.S.U.), University of Chicago, Chicago, Illinois 60637

---

---

## ABSTRACT

Isthmotectal projections in turtles were examined by making serial section reconstructions of axonal and dendritic arborizations that were anterogradely or retrogradely filled with HRP. Two prominent tectal-recipient isthmic nuclei—the caudal magnocellular nucleus isthmi (Imc) and the rostral magnocellular nucleus isthmi (Imr)—exhibited strikingly different patterns of organization. *Imc cells* have flattened, bipolar dendritic fields that cover a few percent of the area of the cell plate constituting the nucleus and they project topographically to the ipsilateral tectum without local axon branches. The topography was examined explicitly at the single-cell level by using cases with two injections at widely separated tectal loci. Each Imc axon terminates as a compact swarm of several thousand boutons placed mainly in the upper central gray and superficial gray layers. One Imc terminal spans less than 1% of the tectal surface. *Imr cells*, by contrast, have large, sparsely branched dendritic fields overlapped by local axon collaterals while distally, their axons nontopographically innervate not only the deeper layers of the ipsilateral tectum but also ipsilateral Imc. Imr receives a nontopographic tectal input that contrasts with the topographic tectal input to Imc.

Previous work on nucleus isthmi emphasized the role of the *contralateral* isthmotectal projection (which originates from a third isthmic nucleus in turtles) in mediating binocular interactions in the tectum. The present results on the two different but overlapping *ipsilateral* tecto-isthmo-tectal circuits set up by Imc and Imr are discussed in the light of physiological evidence for selective attention effects and local-global interactions in the tectum.

**Key words:** tectum, superior colliculus, parabigeminal nucleus, models of attention, stimulus-specific surrounds

---

---

All vertebrates have a complex of nuclei in the isthmus at the pontine-midbrain junction that is intimately interconnected with the optic tectum or superior colliculus. The isthmic complex always receives a topographically organized projection from the ipsilateral tectal lobe, and in amphibians, reptiles, and mammals, it projects topographically to the contralateral tectal lobe. Glasser and Ingle ('78) and Grobstein et al. ('78) showed that this two-stage pathway supports the binocular receptive fields observed in the rostromedial tectum of frogs. But the isthmic complex also projects topographically back to the *ipsilateral* tectum in all

vertebrates. The general function of this ubiquitous return pathway has so far been enigmatic.

The three topographic pathways described above were identified in the course of an earlier HRP study of tectoreticular axons in turtles (Sereno, '85). However, nontopo-

---

Accepted January 21, 1987.

Address reprint requests to Martin Sereno, Division of Biology 216-76, California Institute of Technology, Pasadena, CA 91125.

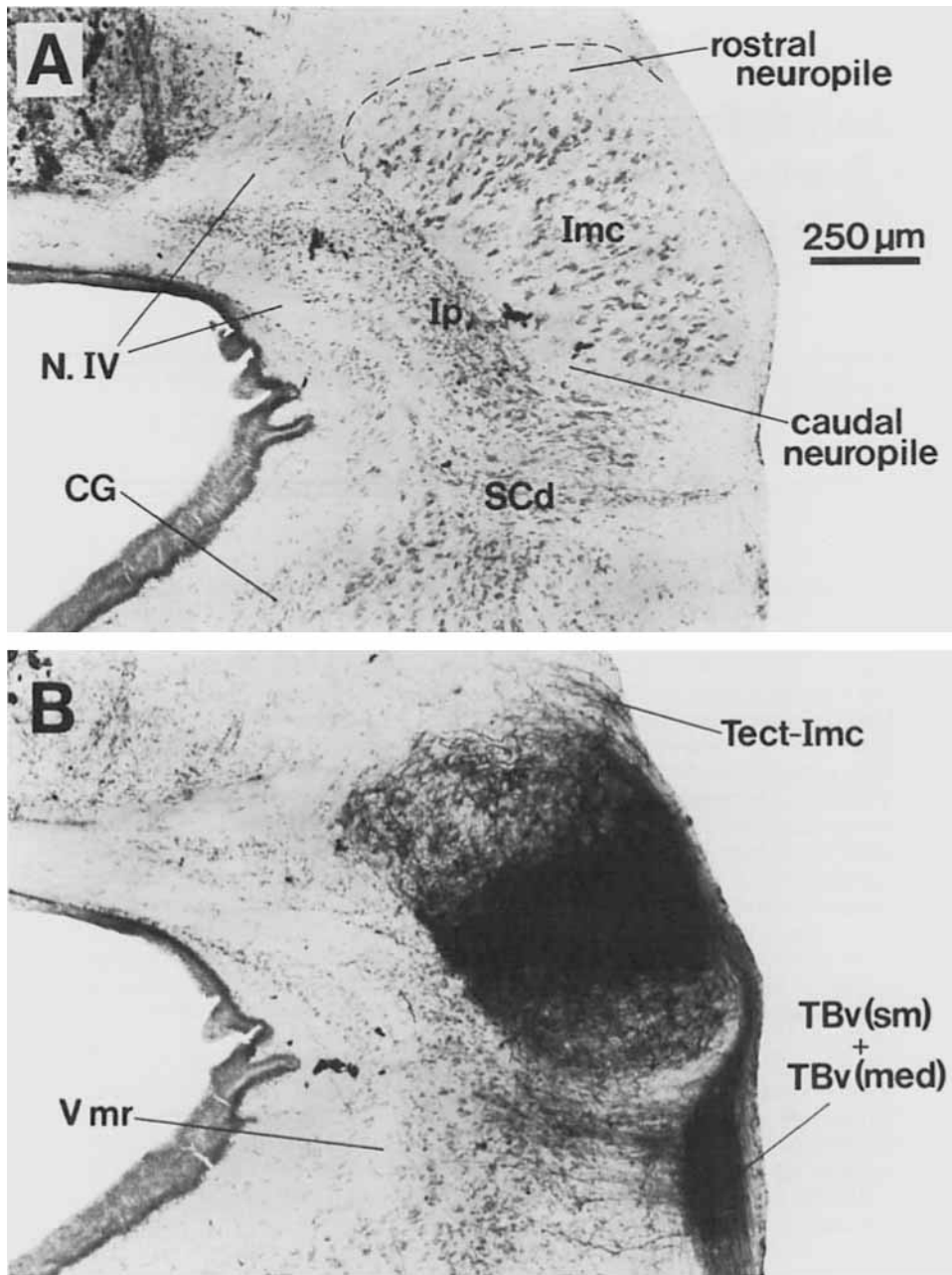


Fig. 1. A: Transverse section through the caudal magnocellular nucleus isthmi (Imc). Note that both the rostral and caudal neuropile layers of Imc (see also Fig. 2) are visible in this section through the middle of the nucleus. The parvocellular nucleus isthmi (Ip), which projects mainly to the contralateral tectal hemisphere, lies just ventromedial to Imc. B: Same-magnification view of Imc after a large but subtotal HRP injection into the ipsilateral tectum. The dark topographic band in Imc consists of a mat of anterogradely

labeled fine-caliber tecto-isthmic terminals superimposed on a cluster of retrogradely labeled Imc cells and their dendritic arborizations. In addition, there is a less dense meshwork of very-large-caliber terminals homogeneously filling the entire nucleus. Ventral to Imc, horizontally directed collaterals arise and terminate in the dorsal part of the small-celled nucleus (SCd); this nucleus projects to the contralateral retina.

graphic labeling also appeared in the topographically organized caudal magnocellular nucleus isthmi (Imc) and in a nearby tectal-recipient nucleus identified as the rostral magnocellular nucleus isthmi (Imr), suggesting that ipsilateral isthmotectal circuits had additional, as yet unrecognized, components. This paper examines the organization of the isthmic complex in turtles, with an emphasis on its ipsilateral relationships. The topographic caudal isthmotectal projection is treated first. Second, the nontopographic rostral isthmotectal projection is considered. The possible

involvement of these ipsilateral pathways in spatial selective attention and local-global computations is then explored.

#### MATERIALS AND METHODS

Twenty-five pond turtles (*Pseudemys scripta*) weighing 0.5–1.5 kg were used. Animals were anesthetized with a small (0.3 ml/kg) dose of Brevital (Wang et al., '77) and then placed in ice for surgery. A craniotomy was performed and a micropipette was introduced into the tectum. In six ani-

Abbreviations

cEnt	Caudal entopeduncular nucleus
CG	Central gray
dLFB	Dorsal peduncle of the lateral forebrain bundle
ICo	Intercollicular nucleus
i-IT	Ipsilateral isthmotectal tract (from Imc)
Imc	Caudal magnocellular nucleus isthmi
Imlf	Interstitial nucleus of the medial longitudinal fasciculus
Imr	Rostral magnocellular nucleus isthmi
Ip	Parvocellular nucleus isthmi
Ipd	Dorsal interpeduncular nucleus
Ipv	Ventral interpeduncular nucleus
Mes V	Mesencephalic trigeminal nucleus
MFB	Medial forebrain bundle
MLF	Medial longitudinal fasciculus
Nmlf	Nucleus of the medial longitudinal fasciculus
N. IV	Trochlear nerve
OT	Optic tract
Pa	Paraventricular hypothalamic nucleus
PC	Posterior commissure
PMc	Profundus mesencephali caudalis
PMr	Profundus mesencephali rostralis
PMv	Profundus mesencephali ventralis
PR	Prerubral area
Re	Nucleus reuniens
RN	Red nucleus
RSL(dm)	Reticularis superioris lateralis, dorsomedial segment
RSI(vl)	Reticularis superioris lateralis, ventrolateral segment

Rsl	Lateral superior raphe nucleus
RSM	Reticularis superioris medius
Rsm	Medial superior raphe nucleus
SAC	Stratum album centrale
Sed	Small-celled nucleus, dorsal segment
SCv	Small-celled nucleus, ventral segment
SFGS	Stratum fibrosum et griseum superficiale (superficial gray)
SGC	Stratum griseum centrale (central gray)
SGP	Stratum griseum periventriculare (periventricular gray)
SN	Substantia nigra
SO	Stratum opticum
SP	Suprapeduncular nucleus
TBd(lg)	Dorsal tectobulbar pathway, large-caliber component
TBd(sm)	Dorsal tectobulbar pathway, small-caliber component
TBi	Intermediate tectobulbar pathway
TBv(med)	Ventral tectobulbar pathway, medium-caliber component
TBv(sm)	Ventral tectobulbar pathway, small-caliber component
Tect-Imc	Tecto-isthmus tract (to Imc)
Torc	Torus semicircularis, central nucleus
Torl	Torus semicircularis, laminar nucleus
TTh	Tectothalamic tract
vLFB	Ventral peduncle of the lateral forebrain bundle
VTA	Ventral tegmental area
x-IT	Crossed isthmotectal tract (from Ip)
III	Oculomotor nucleus
V mr	Mesencephalic root of the trigeminal nerve

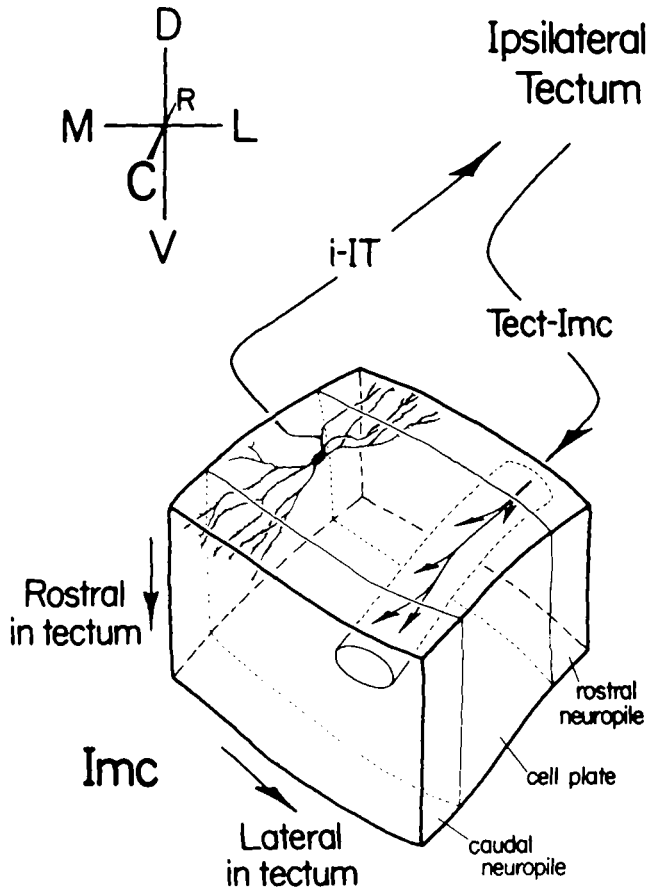


Fig. 2. Schematic diagram of the organization of caudal magnocellular nucleus isthmi (Imc). The nucleus consists of a thick, tilted cell plate faced by rostral and caudal neuropile layers into which the dendrites of Imc cells extend. Spatially restricted rodlike tecto-isthmus afferents (Tect-Imc) penetrate the nucleus perpendicular to the cell plate. The reciprocal point-to-point mapping between the tectum and Imc is arranged so that ventral in the cell plate corresponds to rostral in the tectum while lateral in the cell plate equals lateral in the tectum.

mals, multiple iontophoretic injections (2–3  $\mu$ A for 20 minutes at each site) of concentrated Sigma type VI HRP in pH 8.6 Tris buffer were made at 2 to 4 sites in one tectal hemisphere. Thirteen other animals received small iontophoretic injections (1  $\mu$ A pulsed for 20–100 seconds with a 5–30  $\mu$ m I.D. tip) at a single site or at two widely separated sites. Six animals received large pressure injections (0.5  $\mu$ l) in the medial or lateral half of the pontine tegmentum.

Animals survived for 3 days at 20°C before intracardial perfusion with phosphate-buffered saline followed by a buffered solution containing 1% paraformaldehyde and 3% glutaraldehyde. Gelatin-embedded brains were soaked in 30% sucrose and sectioned the next day on a freezing microtome at 110 or 120  $\mu$ m. Transverse or horizontal serial sections were processed as described in Adams ('77) and counterstained with cresyl violet.

Low-power reconstructions of injection sites, labeled somata, and axon terminals were made from serial sections with a drawing tube. A stereogram of labeled somata was made by hand (Glenn and Burke, '81; Sereno, '85) for one of the horizontally sectioned double injection cases. It can be viewed by ocular divergence or by using a standard stereo viewer (note: fusion attained by crossed-eye viewing will result in inverse depth). In cases with small injections, single HRP-filled axonal and dendritic arborizations were reconstructed with a drawing tube from a number of adjacent sections under a 100 $\times$  oil objective to illustrate their detailed morphology (see Sereno, '85, for details). Nomenclature of cell groups and fiber tracts is the same as that used in Sereno ('85).

RESULTS

Cytoarchitecture of the isthmus complex

The isthmus complex in turtles contains three cytoarchitecturally distinct nuclei—caudal and rostral magnocellular nucleus isthmi, and parvocellular nucleus isthmi. The caudal magnocellular nucleus isthmi (Imc) is a prominent nucleus at the caudal border of the midbrain with a reniform profile in transverse sections (Fig. 1A,B). It consists of a thick plate of cells oriented approximately perpendicular

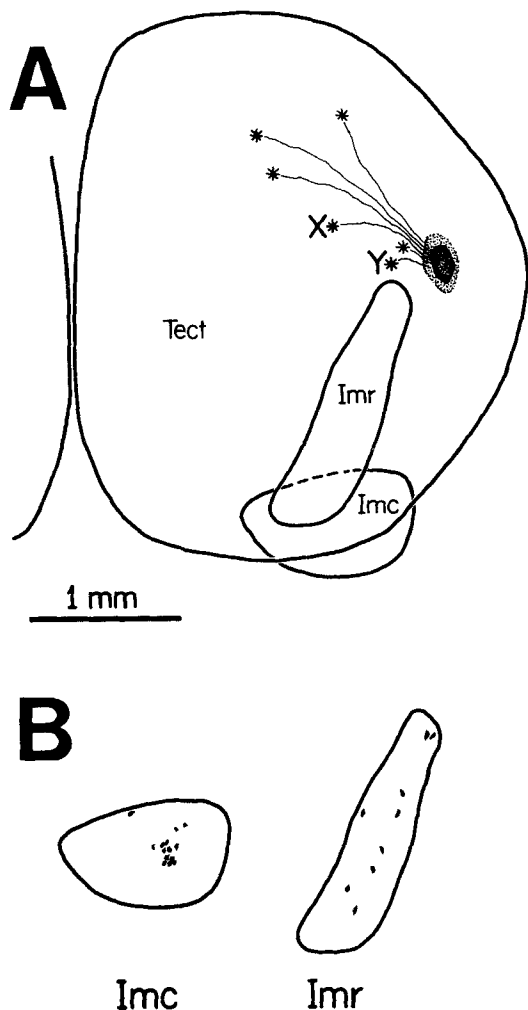


Fig. 3. A: Horizontal reconstruction of a tectal injection. The tectum, the caudal magnocellular nucleus isthmi (Imc), and the rostral magnocellular nucleus isthmi (Imr) were reconstructed from serial transverse sections. This is a stereotaxic view with no correction for the curvature of the tectum. A small HRP injection retrogradely filled 14 cells in a small region of Imc and nine cells scattered throughout Imr. B: Imc and Imr redrawn at the same scale to show the location of the labeled cells. In addition, the injection anterogradely labeled a total of six dense, localized terminal arbors in the tectum (asterisks in A—drawn to scale) rostromedial to the injection site. Their parent axons were about  $3\ \mu\text{m}$  in diameter and coursed through the SGC from the injection site without branching. These terminals most likely arise from Imc neurons (see text). Two of the arbors (at X and Y) are reconstructed at high magnification in Figures 5 and 6.

to the rostrocaudal axis of the brainstem. The dorsal and lateral edges of the plate tilt caudally (Figs. 2, 7A, 11), so that a single section containing all parts of the cell plate is difficult to obtain in either the horizontal or the transverse planes. Neuropile layers adjoin the rostral and caudal faces of the cell plate (Fig. 2). The tilt just noted makes both the caudal and rostral neuropile layers visible in some transverse sections (Fig. 1B; dotted lines in Fig. 11). The cell plate contains compactly arranged, medium-sized, elongated somata ( $9\text{--}15\ \mu\text{m}$  wide,  $18\text{--}25\ \mu\text{m}$  long).

The rostral magnocellular nucleus isthmi (Cruce and Nieuwenhuys, '74) is a rostrocaudally oriented tube of large cells that borders directly on the lateral edge of the superficial layers of the tectum. It is  $1,000\text{--}1,500\ \mu\text{m}$  long, beginning near the caudal face of the tectum just dorsal to Imc

and ending about midway through the tectum (Fig. 3A). In transverse sections, Imr appears as a loose grouping of neurons with robust, elongated somata ( $20\text{--}30\ \mu\text{m}$  wide,  $30\text{--}40\ \mu\text{m}$  long) that is completely surrounded by a cell-free neuropile layer (Fig. 13A). The medium-caliber component of the ventral tectobulbar pathway (TBv[med]) and the ipsilateral Imc-tectal pathway (i-IT) pass just medial to Imr while the small-caliber component of the ventral tectobulbar pathway (TBv[sm]) and the tectoisthmic pathway (Tect-Imc) pass through it (Fig. 13A, B; see also Sereno, '85). Imr has been given other names since it was identified by Cruce and Nieuwenhuys ('74). Foster and Hall ('75), ten Donkelaar and Nieuwenhuys ('79), and Wang et al. ('83), for example, labeled it "nucleus profundus mesencephali," while Brauth et al. ('83) and Künzle and Schnyder ('84) label Imr together with Imc as a unitary "nucleus isthmi magnocellularis."

The parvocellular nucleus isthmi (Ip) lies at the medial edge of the neuropile-somata-neuropile sandwich composing Imc. Because of the tilt, Ip is placed a bit rostral to Imc (Fig. 1A; insets in Figs. 8–10). It consists of a close-packed group of smaller elongated somata ( $5\text{--}8\ \mu\text{m}$  wide,  $8\text{--}12\ \mu\text{m}$  long) that are most densely packed near the border with Imc. Künzle and Schnyder ('84) showed that Ip projects to the contralateral tectal hemisphere. The following sections concentrate on the magnocellular nuclei.

#### Caudal magnocellular nucleus isthmi (Imc)

Figure 1B is a transverse view of Imc after a large tectal injection. Such injections resulted in Golgi-like filling of neurons with somata, terminal arbors, or just fibers of passage at the injection site. The dark band in Imc consists of anterogradely labeled fine-caliber tectoisthmic terminals superimposed on retrogradely labeled Imc somata and dendrites. The location of the dense band depended on the locus of the tectal injection. In addition, a lighter meshwork of large-caliber axons and terminal boutons homogeneously fills the entire nucleus. This background labeling of Imc appeared in other cases regardless of what tectal locus was injected. A few labeled cells and terminals were occasionally seen in Ip after large tectal injections.

Figure 3A shows a horizontal reconstruction of a typical small tectal HRP injection that labeled cells in Imc, Imr, and other nuclei not shown, and several different types of terminals in the tectum. One terminal type was morphologically very distinct and always appeared rostromedial to an injection site (e.g., in Fig. 3A, asterisks represent all such terminals found in this case). Each terminal arose from a robust parent axon ( $3\ \mu\text{m}$  diameter) coursing through the stratum griseum centrale and consisted of a dense, localized, cylindrical thicket of several thousand boutons spanning the stratum griseum centrale (SGC), the stratum fibrosum et griseum superficiale (SFGS), and the stratum opticum (SO).

These terminals were identified as terminals of ipsilateral Imc neurons by several pieces of evidence. First, they

Fig. 4. Transverse view of caudal magnocellular nucleus isthmi (Imc) cell. This neuron was labeled by a small ipsilateral tectal injection and then reconstructed from transverse sections. Its medium-caliber ( $3\ \mu\text{m}$ ) myelinated axon arises from the thickest primary dendrite (at open arrow) and passes rostrally into the isthmotectal tract without emitting local collaterals. Dendrites are covered with irregular spicules and arborize mostly in a plane almost perpendicular to the viewer. A perspective box has been drawn around the arborization (see also inset) to make the resultant foreshortening more apparent; the dendritic field is actually a little longer rostrocaudally than mediolaterally.

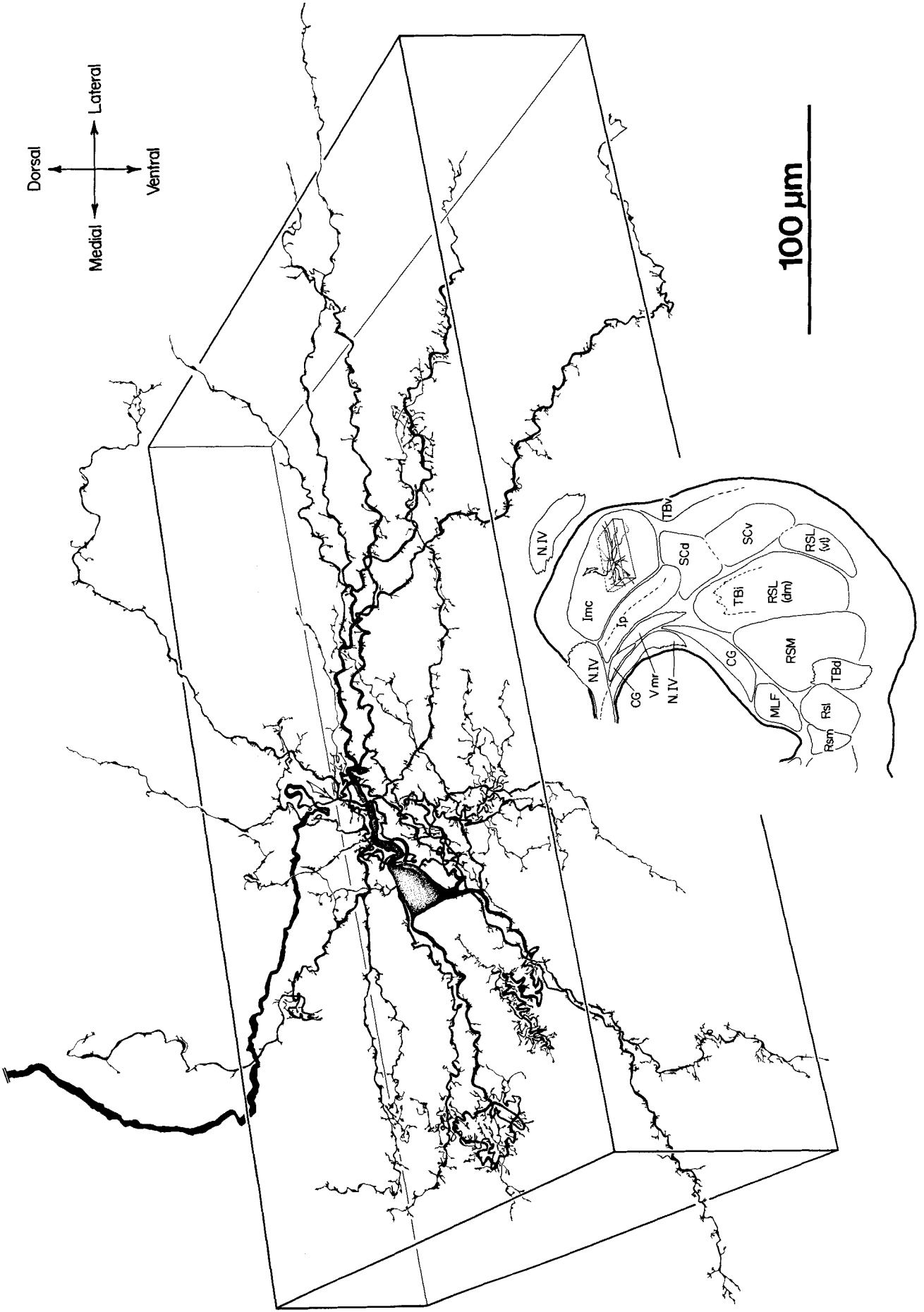
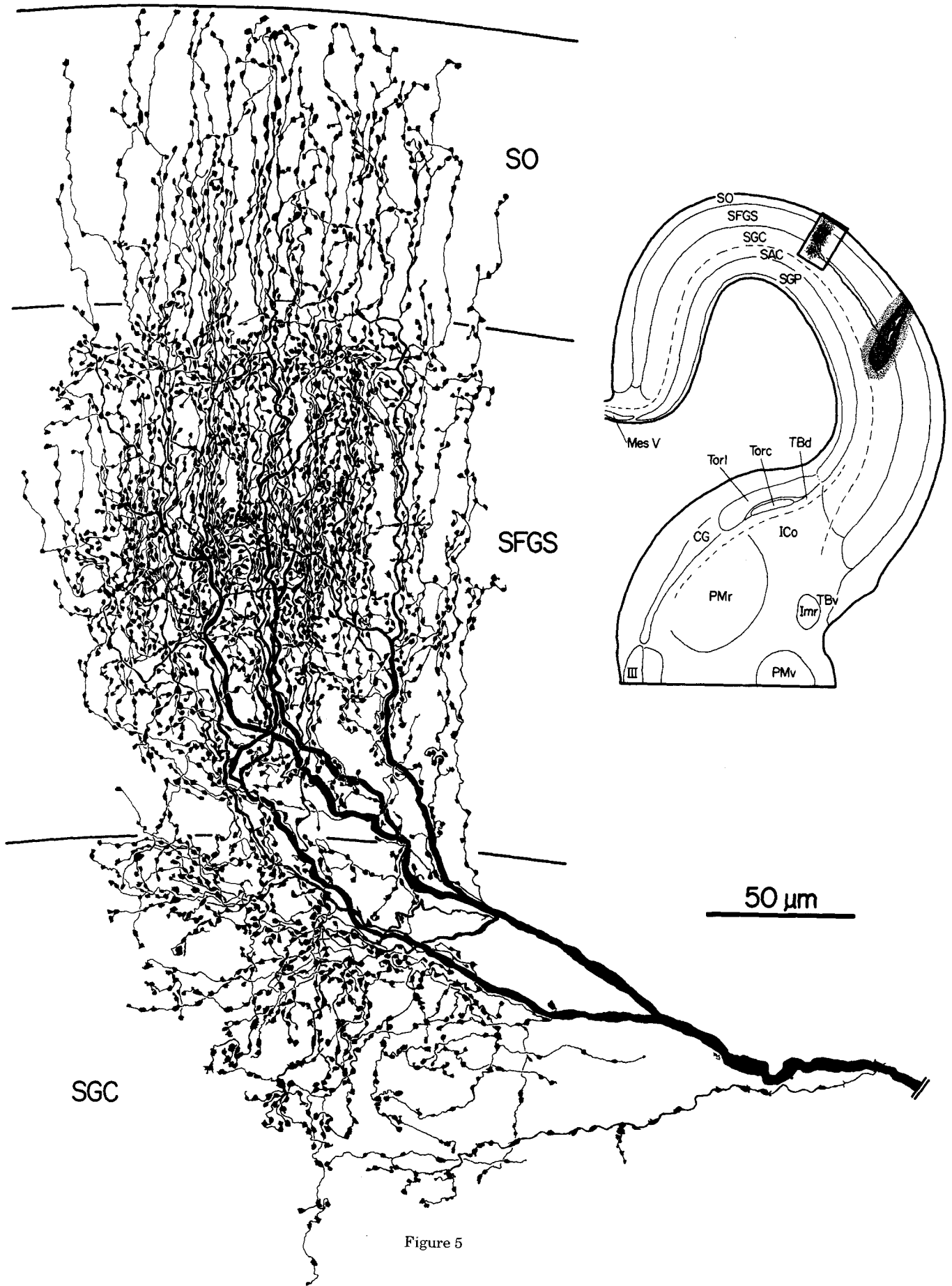


Figure 4



are unlikely to be retinal terminals (e.g., Fig 7E), which avoid the SGC and have parent axons in the stratum opticum. Second, they are not contralateral isthmotectal terminals, which arise from thin (1  $\mu\text{m}$  diameter) axons that cross in the supraoptic decussation, approach the tectum from the front, and then turn caudomedially to run over the tectal surface in the stratum opticum (Fig. 12A,B; insets in Figs. 8, 16). Third, these terminals do not arise from neurons labeled in *Imr*, nucleus lentiformis mesencephali, or profundus mesencephali rostralis (*PMr*). The axons of neurons in those nuclei were reconstructed from serial sections and found to branch widely, sparsely innervating large areas of the tectum. Fourth, the dense thickets are not terminals of thalamic neurons or neurons in the dorsal nucleus of the posterior commissure (*dNPC*) since parent axons of these terminals enter the tectum via the tectothalamic tract (*TTh*). Finally, the parent trunks of these terminals match the diameter and laminar position of the axons arising from *Imc* neurons. Künzle and Schnyder ('84) injected *Imc* with HRP (tetramethyl benzidine development) or a radioactive tracer. In both instances, the laminar distribution of mass label precisely matched that of the dense terminals in the present material. Thus, tectal injections permitted analyses of both the dendritic and axonal arbors of *Imc* neurons.

Large control injections of HRP into the medial or lateral half of the pontine tegmentum left *Imc* as a label-free island surrounded by densely labeled reticular structures. Notably, *Ip* in all these cases was filled with fine-caliber terminals that were particularly dense in the medial third of *Ip* along its border with *Imc*; this label was much denser than the terminal label seen in *Ip* after large, equivalently distant tectal injections.

**Dendritic morphology of *Imc* neurons.** Sixteen *Imc* cells labeled by small tectal injections were completely reconstructed from serial sections. Many more were examined locally or partially reconstructed. Figure 4 is a drawing of an *Imc* neuron made from transverse sections while Figures 8–10 are drawings of horizontally sectioned *Imc* neurons located at dorsal, ventral, and intermediate levels in the nucleus. Figure 7C is a photomicrograph of labeled *Imc* cells.

Four to six primary dendrites radiate from the soma in all directions in the horizontal plane. Secondary and tertiary dendrites turn rostrally or caudally, generating a flattened, elongated dendritic field that extends 500–600  $\mu\text{m}$  rostrocaudally, 150–300  $\mu\text{m}$  mediolaterally, and 75–150  $\mu\text{m}$  dorsoventrally. Consequently, *Imc* dendritic fields are greatly foreshortened in transverse view (Fig. 4) and are seen almost *en face* in horizontal reconstructions (Figs. 7C, 8–10). Viewed on end, a single dendritic field spans roughly 1/50 of the area of the cell plate. One of the primary dendrites is typically more robust than the others (stippled dendrite in Figs. 4, 8, 9). Secondary and tertiary dendrites bear short, filamentous appendages with en passant varicosities that grow more numerous in the rostral and caudal

neuropile layers. The great majority of the varicosities are smaller, more transparent, and have less-regular shapes than putative synaptic boutons arising from HRP-filled axon collaterals in the same material; however, the ends of some dendrites occasionally bear larger, smoother, darker-staining varicosities that are indistinguishable from synaptic boutons (e.g., swellings near asterisk at upper right corner of Fig. 9).

A medium-caliber axon (2.5–3.5  $\mu\text{m}$ ) originates usually from the thick primary dendrite about 50  $\mu\text{m}$  from the soma. After an initial constricted segment that is 20–40  $\mu\text{m}$  long, the axons stain less darkly, except at short, periodically appearing constrictions, suggesting myelination. Local collaterals were never observed in *Imc*. The axons gather into a loose bundle—the ipsilateral isthmotectal tract (*i-IT*)—and exit the dorsomedial corner of the nucleus. The *i-IT* fans out as it approaches the caudolateral face of the tectum, appearing Y-shaped in horizontal sections (inset in Fig. 16). It passes just medial to *Imr* (Fig. 13B) and enters the tectum to run in the upper layers of the SGC. Over 60 *Imc* axons were traced through serial sections until they entered a tectal injection site. In not one instance was an axon collateral observed in the tectum.

**Axon terminal arbors of *Imc* neurons.** The terminal arbors of *Imc* neurons each consist of a conspicuous, dense vertical array of several thousand boutons and are similar at all tectal loci. The myelinated parent axons of these terminals were never observed to emit collaterals before the main trunk turned upward to form the thicketlike arbor. The first vertical branches are myelinated for 100–200  $\mu\text{m}$ . The arbors occupy cylinders approximately 150  $\mu\text{m}$  in diameter and 400  $\mu\text{m}$  tall. A single arbor thus covers about 1/200 of the surface area of one tectal lobe. An average of about 3,000 boutons are packed into each cylinder. The terminal in Figure 5, for example, contained a little more than 2,700 boutons, while the one in Figure 6 contained about 3,600 boutons. There is a characteristic sub-laminar pattern of bouton distribution and size. About 10% of the boutons are located in the SO, about 60% are in the upper two-thirds and 5% in the lower third of the SFGS, and about 25% are in the upper half of the SGC. The boutons in the SGC tend to be larger than those in the SFGS (about 2.5  $\mu\text{m}$  vs. 1.5  $\mu\text{m}$  diameter). Bouton size is quite variable in the upper half of the SO, where a few very large boutons (up to 7  $\mu\text{m}$  in diameter) are mixed in with medium-sized ones. There was little variation in bouton density perpendicular to the main radial axis of an arbor. (The appearance of there being two columns of boutons in the SFGS in the terminal of Figure 6 is the result of a vertical dent in the arbor made by a blood vessel.)

**Topography of the *Imc*-tectal projection.** The topographic organization of the projection from *Imc* to the tectum was assayed at the single-cell level by comparing the dendritic field locations of neurons labeled by two disjunct injections in the same animal. Across-case comparisons based on single injections in different animals were also made. Figure 7A and B show a horizontal reconstruction of a case with two small tectal injections. Photomicrographs of labeled *Imc* cells and sections through each injection site are shown in Figure 7C–E. Individual axons of labeled *Imc* neurons were traced through serial sections to determine which injection site they entered. The labeled neurons form two nonoverlapping clusters in the tilted cell plate of *Imc*. Most of the neurons are located in the lateral third of the cell plate with the dark-outline cluster (injection II) situated

Fig. 5. Axon terminal arbor in the tectum originating from a caudal magnocellular nucleus isthmi (*Imc*) cell. This terminal was labeled by a small tectal injection (see inset) and then reconstructed from several sections. It corresponds to arbor X in Figure 3. The 3  $\mu\text{m}$  diameter myelinated parent trunk emitted no other collaterals before turning upward to give off a radially oriented spray of about 2,700 boutons that were most densely packed in the upper two-thirds of the retinal-recipient SFGS. The boutons in the SGC were somewhat larger (about 2.5  $\mu\text{m}$  diameter) than those in the SFGS (about 1.5  $\mu\text{m}$  diameter).

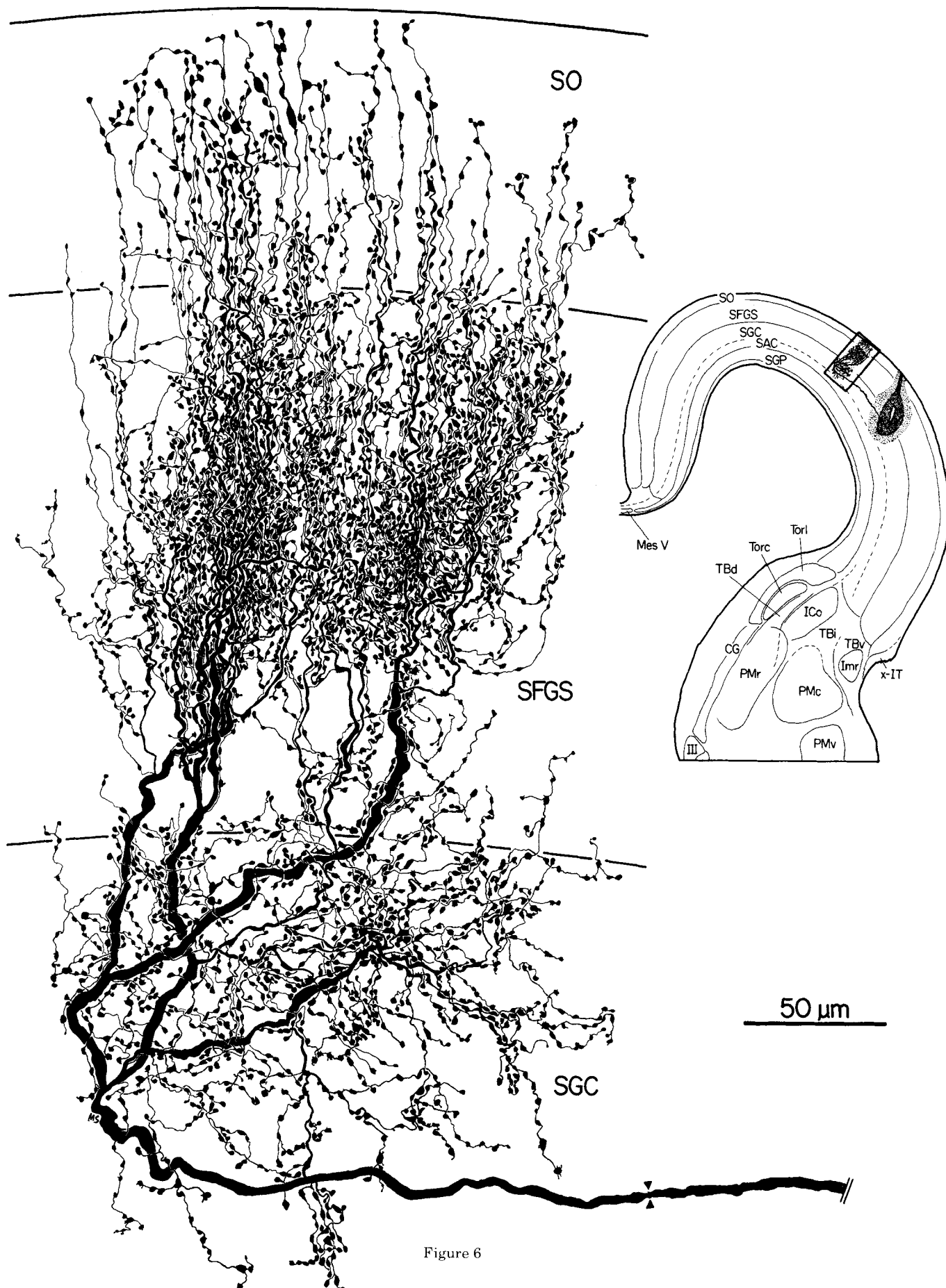


Figure 6

dorsal to (i.e., closer to the viewer than) the less-compact thin-outline cluster (injection D). Several densely filled neurons were reconstructed from serial sections to determine the morphology and location of their dendritic fields. Three of these—labeled 2, 3, and 1 in Figure 7A—are illustrated at high magnification in Figures 8–10. Neuron 2 (Fig. 8) was situated at the edge of the main injection II cluster while neuron 3 (Fig. 9) was at the edge of the main injection I cluster (it was not possible to unambiguously reconstruct neurons in the very center of each cluster). The flattened, elongated dendritic fields of these two neurons are nonoverlapping, though each overlaps with the dendritic fields of many of the neurons in the cluster to which it belongs. An analysis of this and other double injection cases is consistent with a scheme in which rostral in the tectum corresponds to ventral in the Imc cell plate, while lateral in the tectum corresponds to lateral in the cell plate (Fig. 2).

The Imc neurons labeled by injection I are less compactly arranged than the tight cluster of injection II neurons. One of the outlying injection I neurons—neuron 1 in Figure 7A (cell marked with asterisk in Fig. 7C)—was serially reconstructed (Fig. 10). Its dendritic field not only avoids those of injection II neurons but also those of most of its fellow injection I neurons. Two features of injection I are that it invaded the SGC (Fig. 7D) and that it anterogradely labeled ten "ectopic" Imc terminals (asterisks in Fig. 7B and large arrow in Fig. 7D). Injection II, by contrast, was mainly restricted to the SFGS (Fig. 7E) and labeled only one "ectopic" Imc terminal. Thus, it seems likely that some of the ventromedial scatter in the injection I cluster is due to HRP uptake by Imc axons that terminate rostromedial to the injection site.

Comparisons of the loci of labeled Imc cells among cases with single injections confirmed the proposed topography. Figure 11 shows three transversely sectioned cases. Taking into consideration the tilt of the cell plate, increasingly rostral injection sites (B then A then C) result in successively more ventral main clusters while increasingly lateral injection sites (A then B then C) result in successively more lateral clusters. The ventromedial scatter sometimes observed (e.g., in B) is consistent with a fibers-of-passage interpretation. *In summary*, the Imc-tectal projection appears to be a topological, point-to-point mapping in which the dendritic and axon terminal fields of single Imc neurons occupy less than a few percent of the surface of the source and target maps.

### Rostral magnocellular nucleus isthmi (Imr)

Figure 13B is a transverse view of Imr from the same large tectal injection case illustrated in Figure 1B. In con-

trast to the restricted topographic band of labeled cells and terminals observed in Imc, a dense mat of labeled cells and terminals is spread throughout Imr. A similar pattern was observed with injections occupying less than 1% of the tectal surface. The nine Imr cells labeled by the small injection illustrated in Figure 3, for example, were evenly scattered throughout the entire extent of the nucleus. Since scatter occurred no matter what tectal locus was injected, each small patch of the tectum must contain axons from neurons in many parts of Imr.

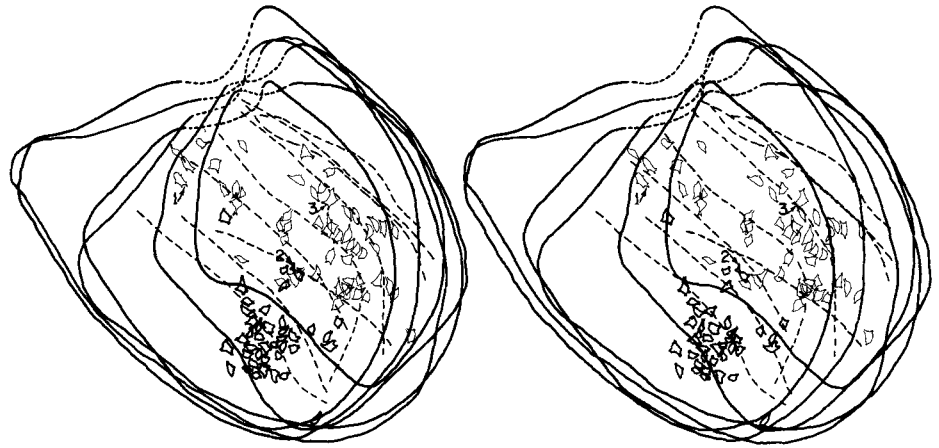
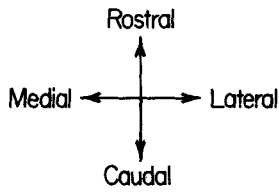
The dense mat of axons in Imr contained three components: fine-caliber fibers passing through without branching, many fine-caliber preterminal branches bearing small-diameter boutons that often contacted Imr cells (Fig. 12C), and large-caliber preterminal branches bearing robust boutons (Fig. 12D,E). Single neuron reconstructions showed that the fine-caliber fibers consist partly of TBV(sm) and Tect-Imc axons (Sereno, '85) while the large boutons arise from the local collaterals of Imr axons (see below). The presence of dense, fine-caliber terminal degeneration in Imr after tectal lesions (Sereno, '85; Foster and Hall, '75) and the labeling of only fine fibers after large tegmental injections suggest that the small boutons represent a tectal input to Imr and not a retrogradely labeled branched input to Imr and the tectum originating from somewhere else. By contrast, the nontopographic background label in Imc described initially (Fig. 1B) turned out to be a retrogradely labeled branched input to Imc and the tectum originating from Imr.

**Dendritic and local axonal morphology of Imr neurons.** Thirteen Imr cells labeled by small tectal injections were completely reconstructed from serial sections. A much larger number were examined in single sections or partially reconstructed. Figure 14 is a reconstruction of an Imr neuron and its local collaterals made from transverse sections, while Figures 16 and 18 are reconstructions of Imr neurons made from horizontal sections. Imr neurons have robust rostral and caudal primary dendrites that arise from an elongated soma and branch only once or twice, giving rise to a large, sparse dendritic field 750–1,000  $\mu\text{m}$  long, 200–300  $\mu\text{m}$  wide, and 200–300  $\mu\text{m}$  deep that approaches the size of the entire nucleus (note the lower magnification of the Imr reconstructions compared to those of Imc cells). Distal dendrites often extend medially through the Imr neuropile to reach profundus mesencephali caudalis. All secondary and tertiary dendrites were covered with short, uniform hairlike spicules quite unlike the longer, irregular appendages seen on distal Imc neuron dendrites.

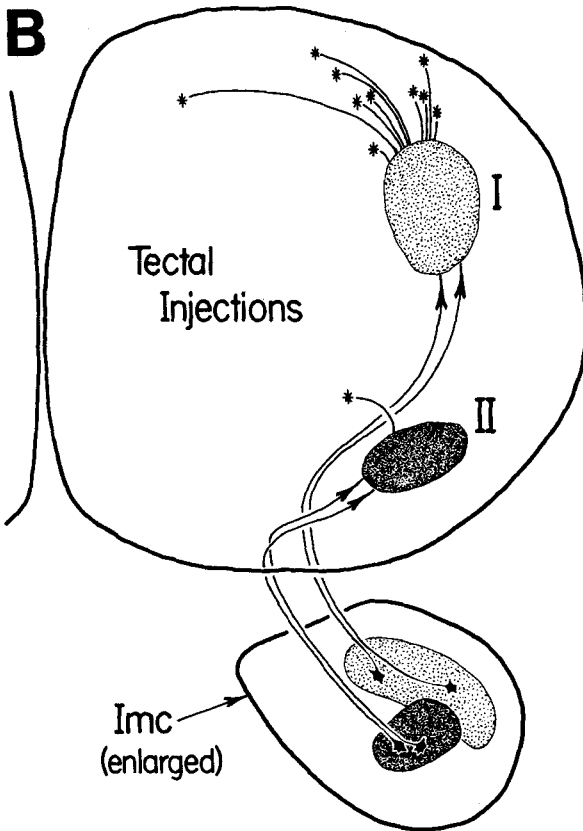
A robust axon (4–6  $\mu\text{m}$  in diameter) originates most often from the rostral primary dendrite a short distance from the soma. The initial branching of the axon appears random (compare Figs. 14, 16, 18), but a pattern emerges when the branches are followed through serial sections. Each Imr neuron gives rise to one or more myelinated trunks to the tectum and one or more myelinated trunks to Imc, which will be described in turn. In addition, a sparse field of local axon collaterals bearing large boutons usually appeared within Imr (e.g., Figs. 14, 18).

**Branches of Imr axons in the tectum.** Figure 15 is a reconstruction of part of one of the branches that reaches the tectum from the Imr neuron illustrated in Figure 14. The axon leaves Imr to enter the SGC (see inset to Fig. 15) about one-third of the way forward from the caudal face of the tectal hemisphere. Preterminal branches (open arrows) are emitted at intervals of about 200  $\mu\text{m}$ . (By contrast, an

Fig. 6. Axon terminal arbor in the tectum originating from caudal magnocellular nucleus isthmi (Imc) cell. This terminal was also labeled by a tectal injection (see inset) and recovered from several sections. It corresponds to arbor Y in Figure 3. The 3,600 boutons in this arbor appear to form two columns, especially in the SFGS. This is the result of a large vertical blood vessel taking a chunk out of a bouton distribution that is otherwise radially homogeneous when viewed from the tectal surface. All nodes on the 3  $\mu\text{m}$  diameter parent trunk situated outside the dense arborization (for example, node at paired triangles) were unbranched.

**A**

— to tectal injection site I  
 — to tectal injection site II

**500 μm****B**

**Horizontal  
Reconstruction**

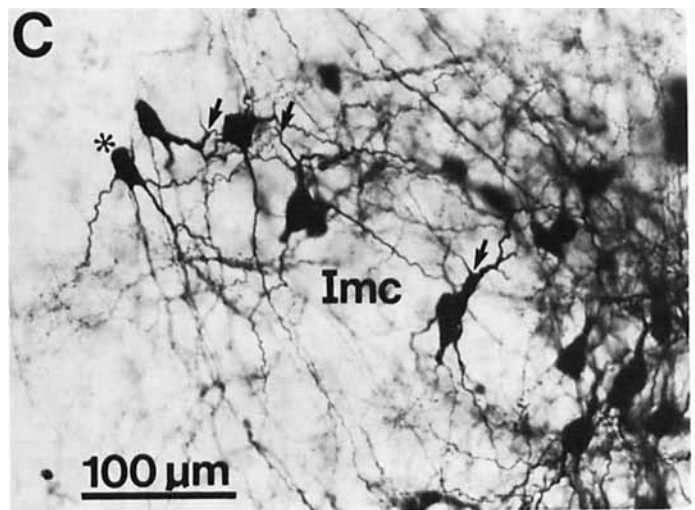
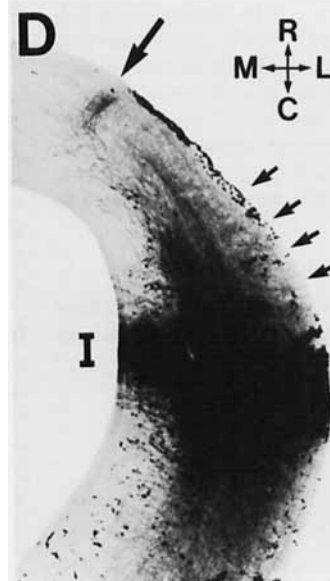
**C****D****E**

Fig. 7. Analysis of a case with two tectal injections. **A**: Stereoscopic view of retrogradely labeled cells in caudal magnocellular isthmi (Imc). Injection II cells (bold outlines) form a tight clump situated dorsal (i.e., near the viewer) to the more diffuse injection I cell cluster (thin outlines). The dendritic arbors of the cells numbered 2, 3, and 1 are reconstructed at higher magnification in Figures 8–10. The tilt of the cell plate (boundaries indicated by dashed lines) is especially obvious when the figure is viewed in stereo by ocular divergence or by using a standard stereo viewer (fusion obtained by cross-eyed viewing will result in inverse depth). **B**: Horizontal reconstruction of the tectal injections and the corresponding labeled clusters of Imc cells. Injection I (light stipple and photomicrograph in **D**) antero-

gradely labeled many more Imc axon arbors (asterisks) than did injection II (dark stipple and photomicrograph in **E**), probably because injection I invaded the SGC, where the myelinated parent trunks of these arbors run. **C**: Photomicrograph of labeled Imc cells in the injection I clump. The cell with an asterisk is cell number 1 in **A** and is reconstructed in Figure 10. The arrows indicate axon origins. **D**: Injection site I. An anterogradely labeled Imc terminal (large arrow) is visible rostral to the injection. The retinal-recipient SFGS and SO, however, are unlabeled rostrally (small arrows). **E**: Injection site II. The retinal terminal layers are heavily labeled around this injection (small arrows).

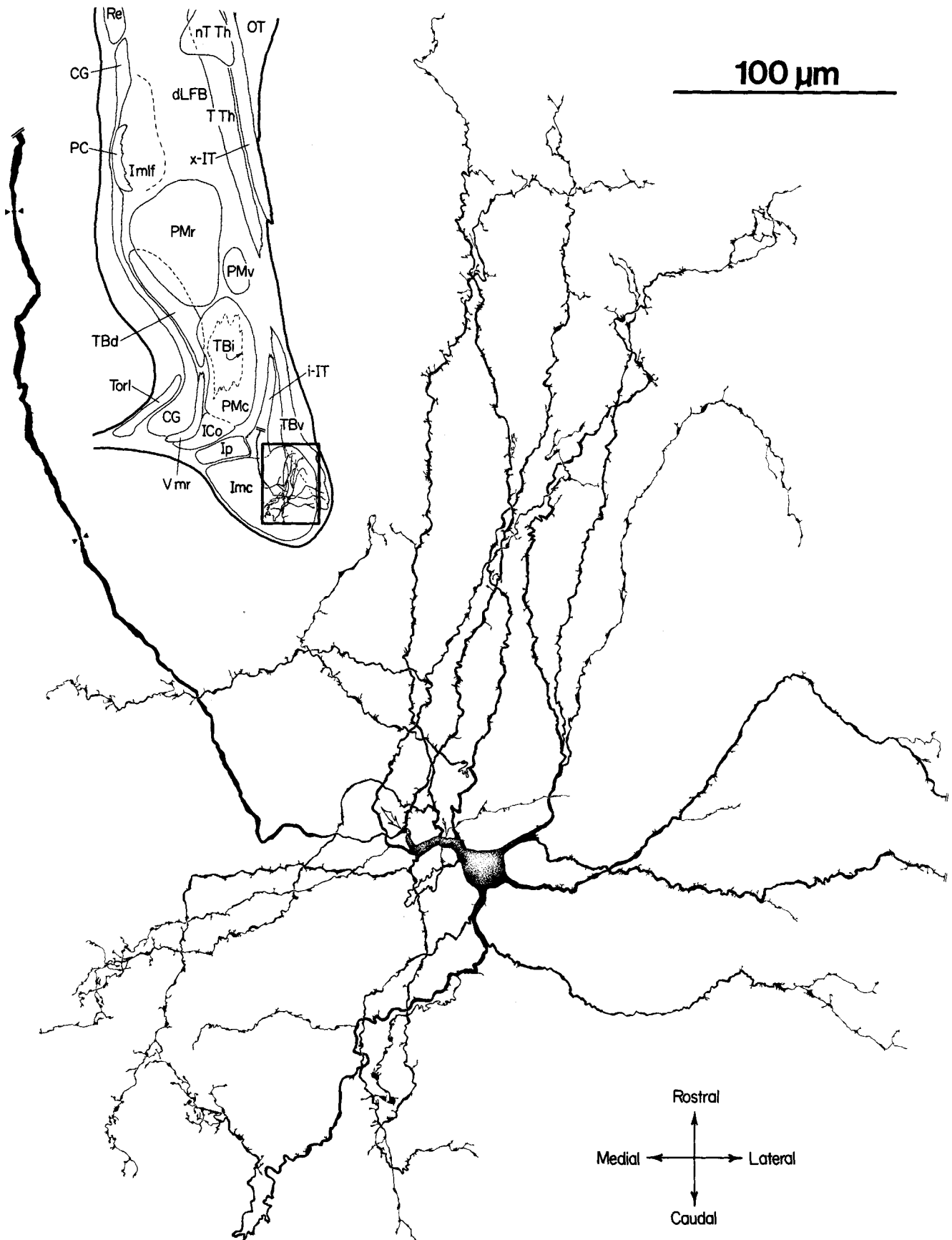


Fig. 8. High-magnification view of caudal magnocellular nucleus isthmi (Imc) neuron number 2 from Figure 7A. This neuron was labeled by tectal injection II (Fig. 7B,E) and reconstructed from horizontal sections, resulting in an *en face* view of the flattened, rostrocaudally elongated dendritic field. The dendrites bear irregular spicules that grow more numerous on the secondary and tertiary branches that penetrate the rostral and caudal neuropile layers. The 3  $\mu$ m diameter axon (origin at open arrow; unbranched nodes at paired triangles) arose from the thickest primary dendrite (stippled) and emitted no collaterals until it entered the tectal injection site. The inset shows the location of the neuron.

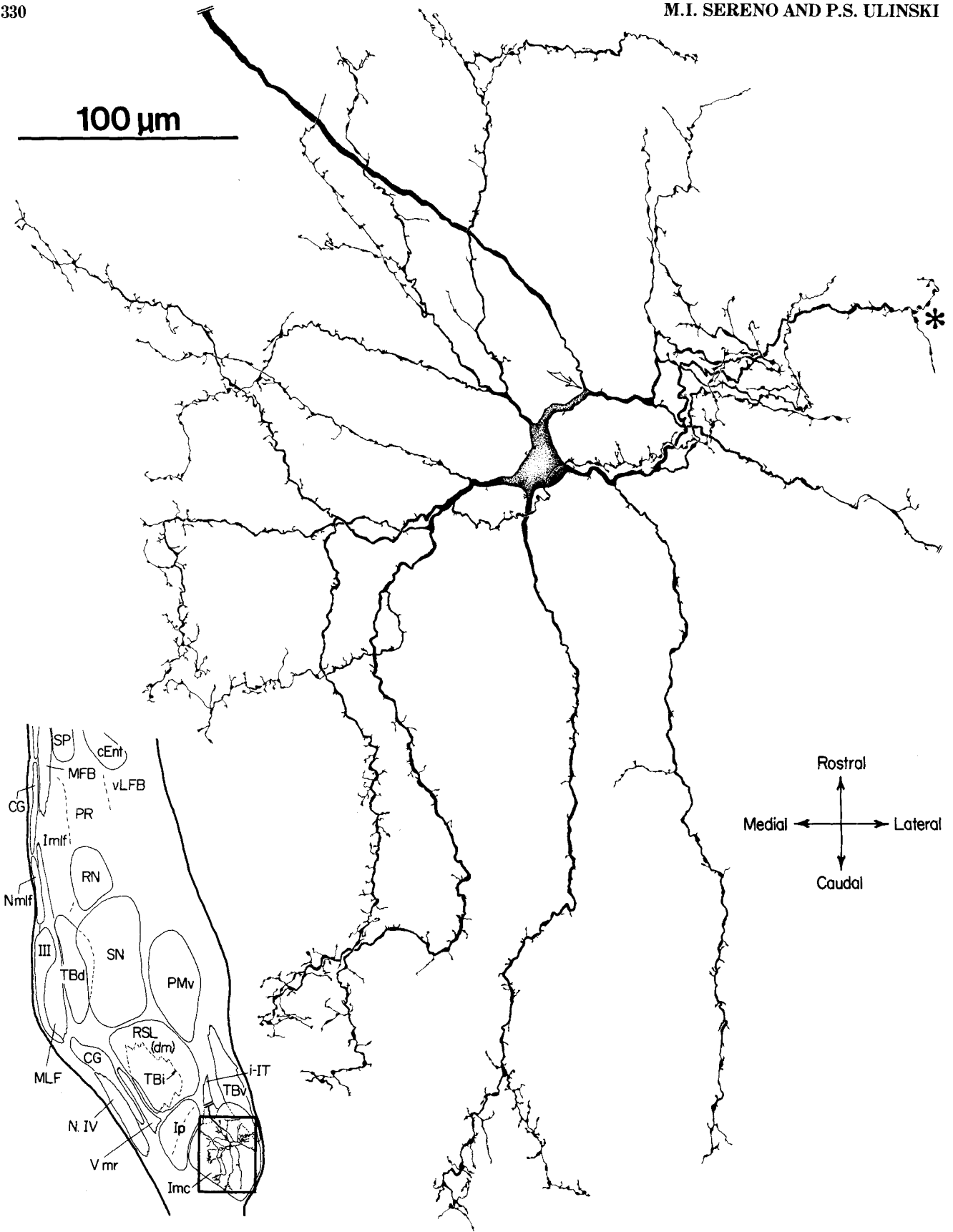


Figure 9

entire Imc terminal arbor is only about 150  $\mu\text{m}$  wide.) These branches course toward the ventricular surface, giving rise to radially oriented strings of 5 to 30 large boutons situated in the lower half of the SGC and in the stratum album centrale (SAC). The main trunk continued to branch until it was lost without any sign of thinning at the injection site. Thicker, apparently myelinated collaterals are given off at some branch points (one at A and two at C). They are almost as thick as the main trunk and course rostrally through the SGC and SAC (3-D arrows) giving off radially oriented strings of boutons into the SGC and SAC at regular intervals. The collateral at A innervated the middle and near rostral tectum while the collaterals at C innervated the rostral tectum, one reaching the extreme rostromedial edge of the tectum. The second branch to the tectum (at upper left in Fig. 14) was similar in morphology to the trunk just described, except that it distributed strings of boutons to the caudal face of the tectum. It was lost near the caudomedial edge of the tectal hemisphere, at which point it had thinned considerably. The tectal branches of other Imr neurons were similar in overall form to the one illustrated in Figures 14 and 15 though sometimes they were a bit less fastidious in covering all parts of the tectum.

**Branches of Imr axons in Imc.** The other target of Imr axons besides the tectum was, unexpectedly, Imc. Figure 17 is a horizontal reconstruction of a single axon terminal arbor that arose from the Imr neuron shown in Figure 16 and terminated in Imc. Typically, Imr neurons give off two or three thick myelinated trunks to Imc that enter either the front face or the medial edge of the cell plate, often at more than one dorsoventral level (for example, neuron in Fig. 18). Once in Imc, each trunk splits into several myelinated branches that wander back and forth, giving off strings of very large (2–3.5  $\mu\text{m}$  diameter) *en passant* boutons that stand out amongst the much smaller (1  $\mu\text{m}$  diameter) boutons found in the terminal arbors of tectoisthmic axons. Terminal boutons of Imr axons are often capped with a tiny varicosity (Fig. 17). A single Imr axon thus sparsely distributes 1,000–2,500 boutons to many mediolateral and dorsoventral levels in the cell plate and the caudal neuropile of Imc. The arbor in Figure 17 contained about 1,840 boutons. The terminal field is rigorously confined to Imc; when a branch comes to the edge of the nucleus, it rarely continues for more than a few microns outside of it before reentering (for example, branch at extreme lower right of arbor in Fig. 17).

The nontopographic nature of a single Imr axon in Imc is brought out by comparing its spatial distribution to that of the restricted clusters of retrogradely labeled Imc cells and anterogradely labeled tecto-isthmic terminals produced by the same injection. In Figure 17, for example, small clusters

of Imc cells and Tect-Imc terminals overlapped in the lateral third of Imc (not illustrated). The Imr axon, by contrast, not only distributed boutons in and around these clusters, but actually somewhat more densely innervated the topographically inappropriate medial half of Imc. Other reconstructions of Imr axons in Imc revealed equally nontopographic bouton distributions.

The uniform background labeling of Imc seen after large tectal injections (Fig. 1B) thus represents a number of Imr axon arbors filled through the tectal branches of their bifurcating axons. Figure 19 is a high-magnification photomicrograph of the upper left-hand corner of Imc from the transverse section shown in Figure 1B. The background label consists of a meshwork of robust, myelinated branches bearing very large boutons that are precisely confined to Imc, clearly marking its boundaries. The morphology and organization of the background terminals labeled by large tectal injections closely matches that of single identified Imr axon arbors in bouton size, lack of topography, and complete restriction to Imc. The lack of nontopographic large-caliber terminal degeneration in Imc after tectal lesions (Serenio, '85) is consistent with this conclusion.

## DISCUSSION

Neurons in the tectal-receiving rostral magnocellular nucleus isthmi (Imr) of the turtle give rise to a strikingly nontopographic output that is superimposed on the topographically organized circuit between the ipsilateral tectum and the caudal magnocellular nucleus isthmi (Imc), not only in the tectum but also in Imc itself. Figure 20 schematically illustrates the morphology of single Imc and Imr neurons. In this section, the organization of Imc and Imr is summarized and compared with findings on similar nuclei in other vertebrates. Some functional implications of these two ipsilateral tecto-isthmo-tectal circuits are then considered.

### Anatomy of isthmotectal neurons

**The caudal topographic nucleus isthmi.** A component of the nucleus isthmi complex that receives a tectal input and projects back to the ipsilateral tectum appears to be present in all vertebrate classes. This nucleus always has a topographic connection with the ipsilateral tectum and often consists of a platelike array of neurons with elongated dendritic fields that project both to the superficial gray layers and to a directly underlying non-retinal-recipient layer in the central gray. In each instance, however, there are differences in detail. In turtles, Imc somata are arranged into a thick cell plate faced with rostral and caudal neuropile layers. The neurons have flattened bipolar dendritic fields covering a few percent of the cell plate area as well as spatially restricted axon arbors covering less than 1% of the ipsilateral tectal hemisphere. The swarm of several thousand boutons typically given off by a single Imc axon occupies not only the superficial retinal-recipient laminae (SO and SFGS) but also part of the underlying central gray (upper half of the SGC). Imc neurons appear to be cholinergic (Desan et al., '84).

In bony fish (Sakamoto et al., '81; Ito et al., '82), nucleus isthmi contains a sharply bounded cell plate (shell) but then only a single, caudal neuropile layer (core) into which the unipolar dendritic arbors of the cell plate neurons extend. Their axon terminals in the tectum innervate the superficial gray and a non-retinal-recipient layer at the top of the central gray. However, many fish species have one or two

Fig. 9. High-magnification view of caudal magnocellular nucleus isthmi (Imc) neuron number 3 from Figure 7A. This neuron was labeled by tectal injection I (Fig. 7B,D). Its flattened, elongated dendritic field volume is entirely ventral to that of the injection II cell illustrated in Figure 8. The 3  $\mu\text{m}$  diameter myelinated axon (origin at open arrow) arises from the thickest primary dendrite (stippled) and emits no local collaterals. Most dendrites bear filamentous spicules; the tip of one dendrite (asterisk), however, gives rise to varicosities morphologically indistinguishable from synaptic boutons as it ends within the ventral tectobulbar tract (TBV—see inset).

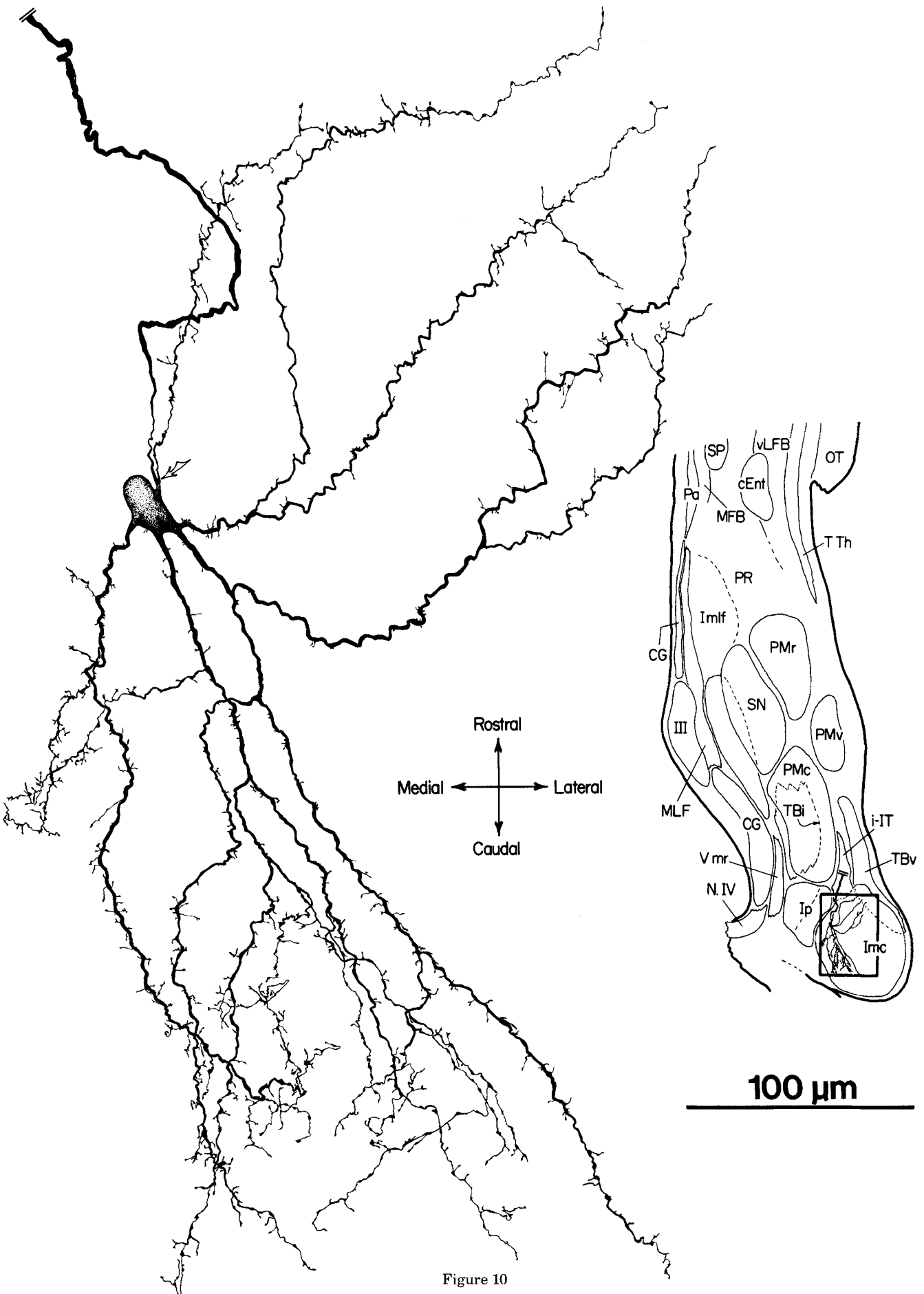


Figure 10

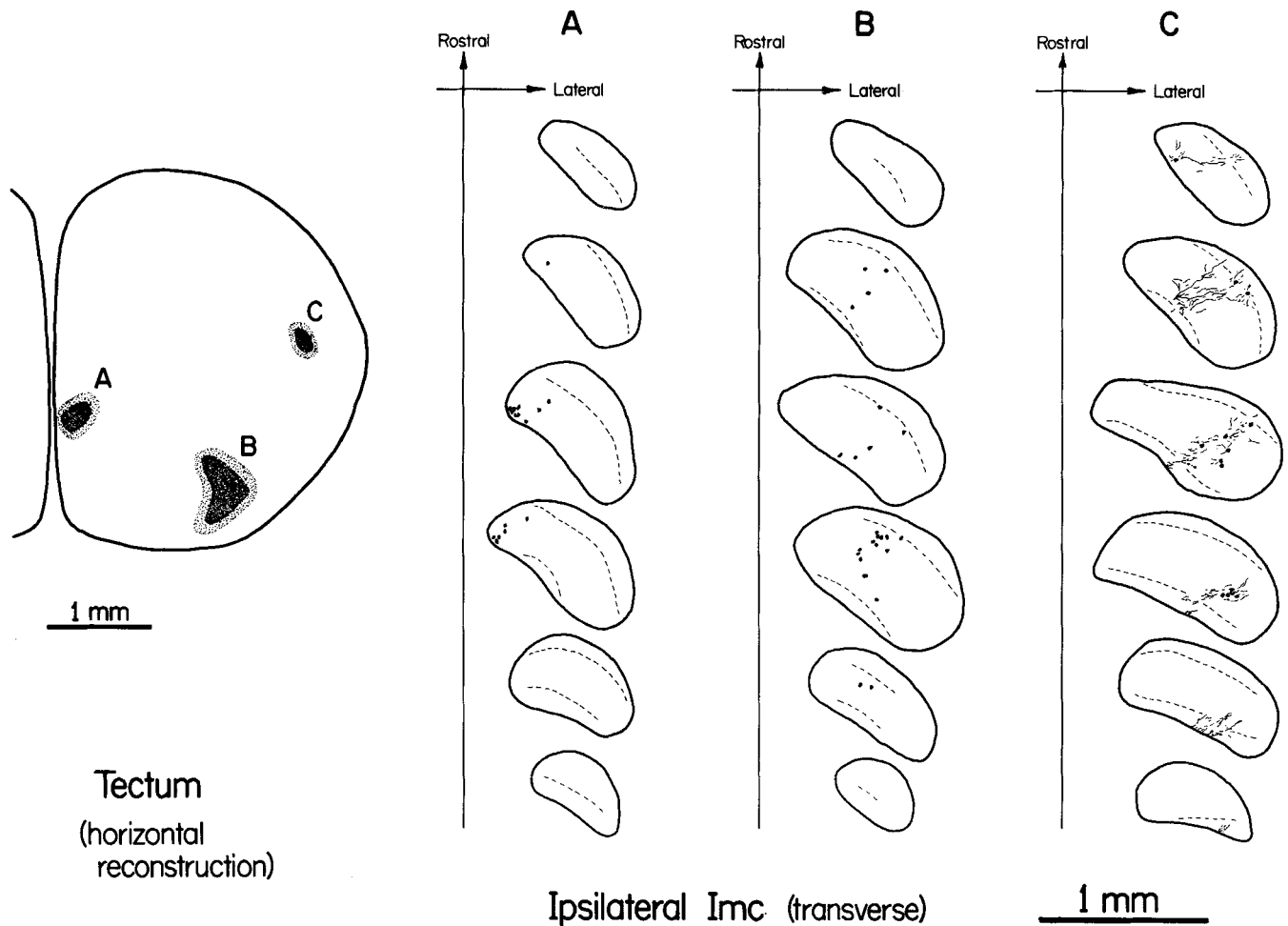


Fig. 11. Labeled caudal magnocellular nucleus isthmi (Imc) neurons in three transversely sectioned cases each with a single tectal injection. Taking account of the tilt of the Imc cell plate (dorsal and lateral edges caudal to its ventral and medial edges), increasingly rostral tectal injections (B then A then C) are seen to result in more and more ventral clusters in the cell plate, while increasingly lateral injections (A then B then C) give more and more lateral clusters. The ventromedial scatter of labeled Imc cells in case B is consistent with a fibers-of-passage interpretation using that scheme; some of the Imc axon trunks, which stream rostromedially through the central gray of the tectum, must have been filled at the injection site before they terminated. The dashed lines in Imc indicate the boundaries of the cell plate with rostral and neuropile layers. In case C, the dendritic arbores of the labeled cells were also drawn. No correction was made for the curvature of the tectum in the horizontal reconstructions of the injection sites.

additional even deeper layers of retinal terminals in the middle and lower parts of the central gray (Vanegas et al., '84). Some of the contacts made by isthmotectal terminals

Fig. 10. High-magnification view of "ectopic" caudal magnocellular nucleus isthmi (Imc) neuron number 1 from Figure 7A. This neuron was labeled by tectal injection (Fig. 7B,D). Unlike many other injection I neurons whose dendritic field volumes overlap each other ventrally and laterally in the nucleus (see, for example, neuron 3 illustrated in Fig. 9), this neuron's dendritic field occupies the most medial part of the nucleus (Fig. 7C), overlapping few other labeled dendritic fields to a significant degree. It was probably injected as a fiber of passage whose terminal arborization lies rostral and medial to the injection site (possibly one of the ten "ectopic" arbores shown beyond injection I in Fig. 7B,D). A 3 μm diameter myelinated axon arises (open arrow) from the base of a dendrite and makes a semicircular detour around a blood vessel soon after becoming myelinated. The inset shows the location of the neuron.

may be axoaxonic synapses on retinal terminals (Henley et al., '86). A contralateral isthmotectal projection is apparently lacking.

In frogs, a loosely packed cell plate and its associated neuropile layers (medulla) are almost completely enclosed by a unique, tightly-packed sheet of cells (cortex) resulting in a mediolaterally oriented tacolike structure (Gruberg and Udin, '78; Grobstein and Comer, '83). Part of the medulla and part of the anterior limb of the cortex project to the ipsilateral tectum. Ipsilateral isthmotectal axons terminate throughout the superficial retinal-recipient zone (layers A-F), but also just below it (layer 8) (Gruberg and Udin, '78; Gruberg and Lettvin, '80). As with bony fish, some frog species (for example, *Rana pipiens*) have an even

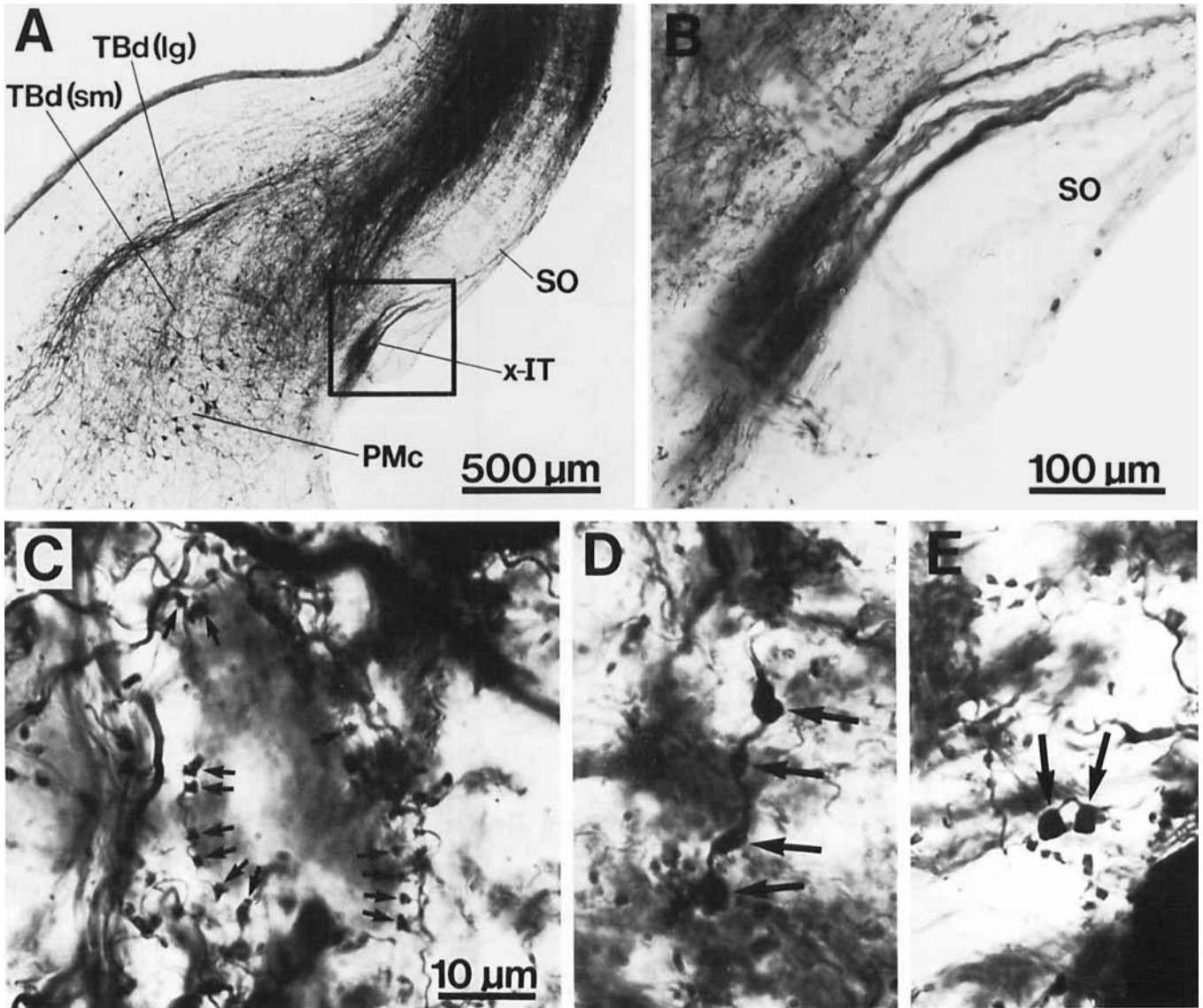


Fig. 12. A: Photomicrograph of the lateral border of the tectum in transverse section showing the crossed isthmotectal tract (x-IT). It was retrogradely labeled by a large tectal injection (not shown) that also heavily labeled other tectal afferents (for example, from profundus mesencephali—PMc) and tectal efferent pathways (for example, the large- and small-caliber dorsal tectobulbar pathways—TBd[lg] and TBd[sm]). The x-IT arises from parvocellular nucleus isthmi (Ip in Fig. 1A), passes rostrally to cross in the supraoptic decussation, and then caudally to approach the rostralateral edge of the contralateral tectum. When a fascicle of x-IT fibers reaches the appropriate rostrocaudal point along the edge of the tectum, it turns upward abruptly (shown here) to run over the tectal surface in the stratum opticum (SO) until it reaches the mediolateral locus where it terminates. B: High-magnification view of x-IT (boxed region in A) showing fascicles of fine-caliber axons (about 1  $\mu$ m diameter). C: High-magnification view of Imr (see Fig. 13B for low-power view) showing putative contacts (arrows) between small-diameter synaptic boutons and an unlabeled, Nissl-stained Imr cell soma. These boutons were labeled after a large tectal injection and probably represent a tectal input to Imr (see text). D,E: Smaller numbers of very-large-caliber boutons (arrows) also appeared in Imr (same magnification as C). These probably arise from local collaterals of Imr cells (see Figs. 14, 16).

deeper lying retinal terminal layer in the central gray (layer G) (Lazar, '84). Nucleus isthmi appears to be cholinergic in frogs (Desan et al., '84). The contralateral isthmotectal projection arises not only from the posterior limb and ventral folded part of the tectal cortex but also from the medulla.

In snakes, the somata and dendrites of nucleus isthmi neurons are not organized into obvious cell plate and neuropile layers. More notable, however, are the small terminal arbors of these neurons, which bypass not only the SGC but also the SFGS to terminate in only the most superficial of the retinal-recipient laminae—the SO—and in the over-

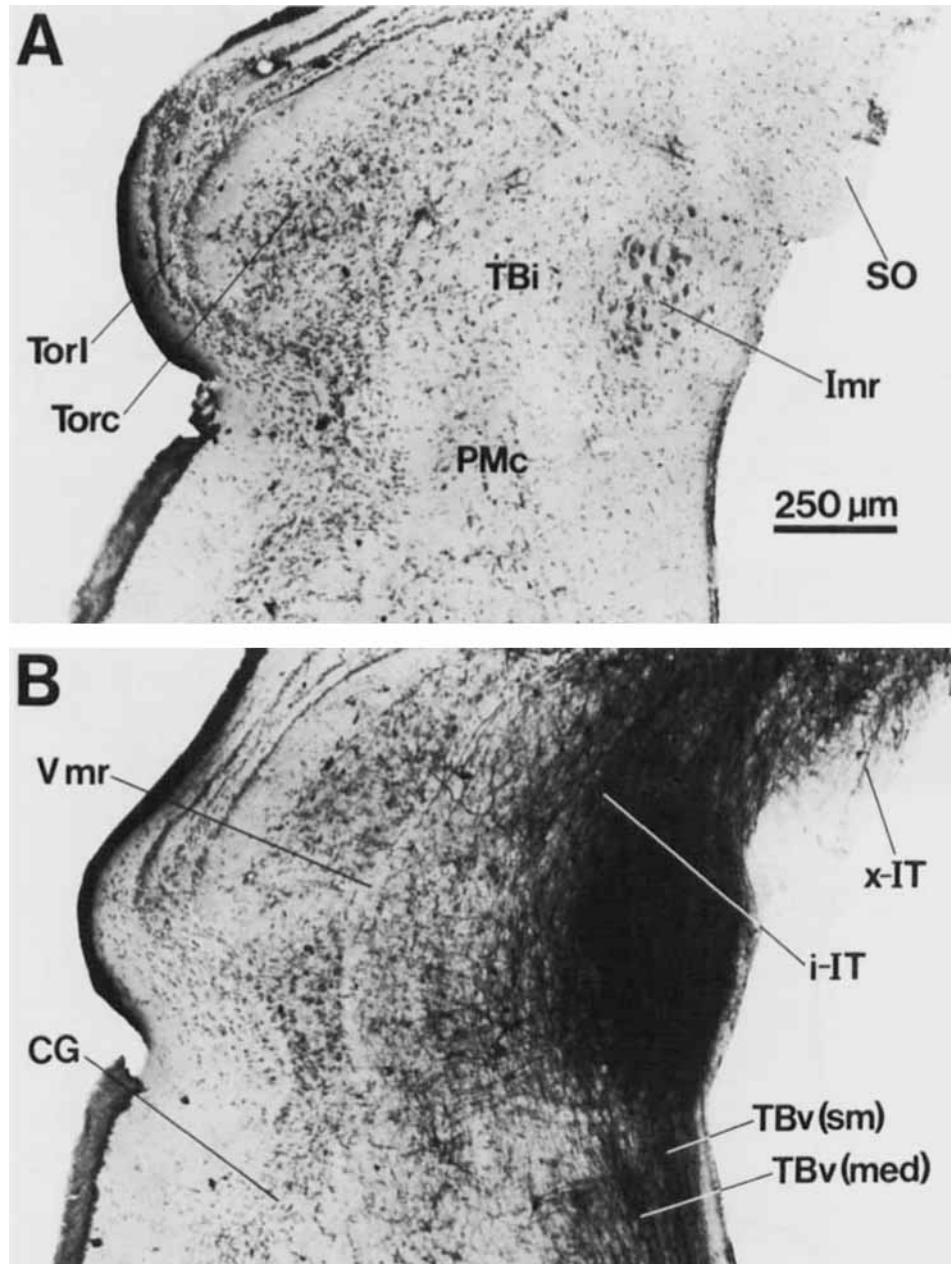


Fig. 13. **A:** Transverse section through the rostral magnocellular nucleus isthmi (Imr). The large somata in Imr form an oval cluster that is completely surrounded by a neuropile layer. **B:** Same-magnification view of Imr after a large but subtotal HRP injection into the ipsilateral tectum (same case as in Fig. 1B). The dark blob that completely engulfs Imr in this and most other sections through the nucleus consists of a mass of fine-caliber terminals probably from the tectum (see text and Fig. 12C) superimposed on a cluster of labeled Imr cells, their dendrites, and the robust local collaterals arising from their large-caliber axons. In addition, the small-caliber component of the ventral tectobulbar pathway, TBv(sm), passes directly through Imr without branching (Serenó, '85). The ipsilateral isthmotectal tract (i-IT) and the medium-caliber component of the tectobulbar pathway, TBv(med), pass Imr medially.

lying stratum zonale (Dacey and Ulinski, '86b). In this respect, snakes appear to differ from all other vertebrates (as they do in having the dendrites of their principal deep-layer tectobulbar cell types end before entering any of the retinal-recipient laminae—Dacey and Ulinski, '86a). Contralaterally projecting isthmotectal neurons are intermixed with ipsilaterally projecting ones.

In birds, the nucleus similar to turtle Imc is the parvicellular nucleus isthmi, Ipc. It lacks differentiated neuropile layers but otherwise conforms to the general vertebrate pattern in that cells with elongated dendritic fields innervate the superficial retinal-recipient layers 2–5 (=IIb–d) as well as directly underlying non-retinal-recipient layers 10 and 11 (=IIi) (Cajal, 1899; Hunt et al., '77). The dense nest

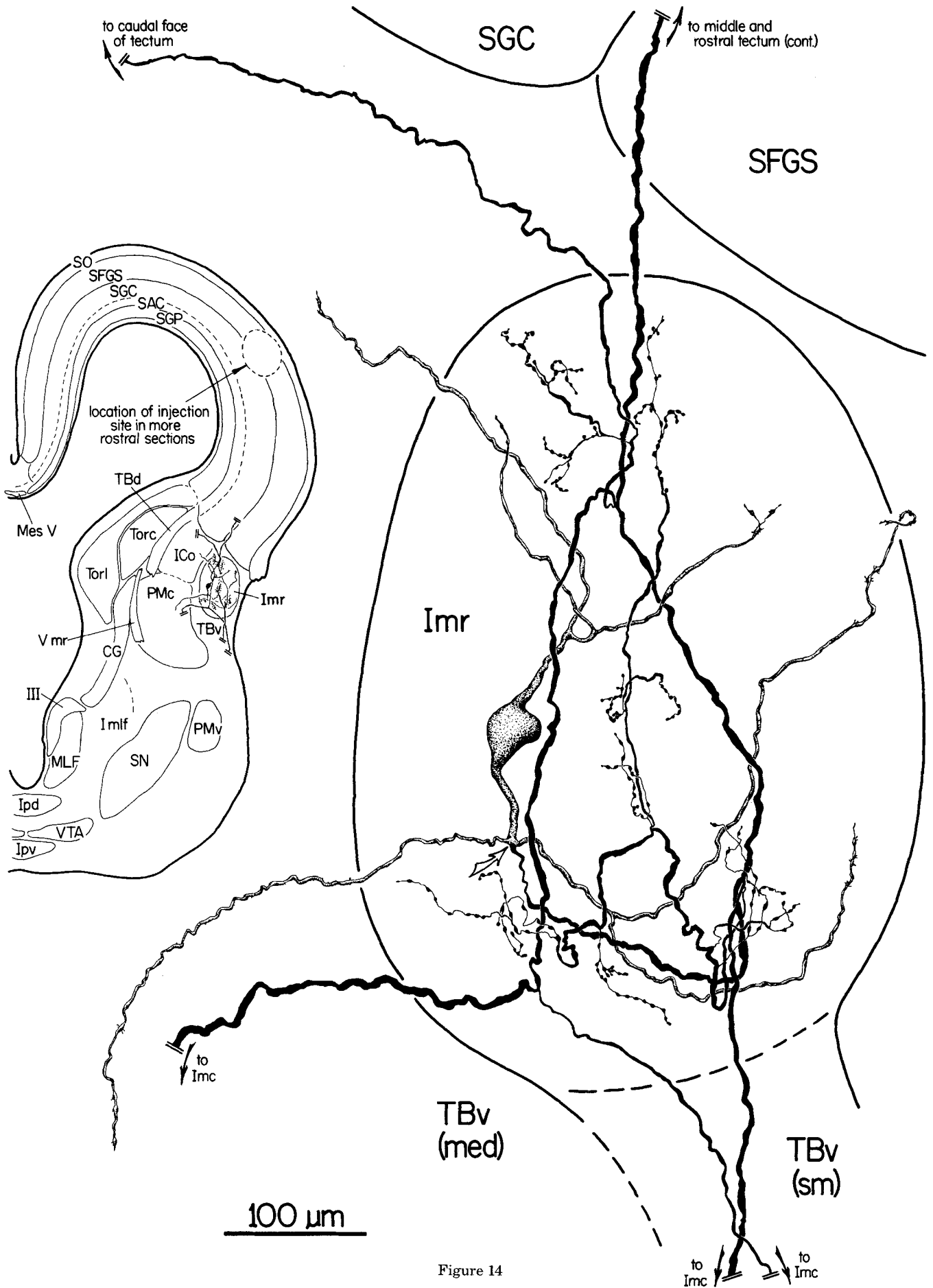


Figure 14

of boutons in each Ipc terminal is confined to a narrower cylinder than turtles. Hunt et al. ('77) showed that Ipc terminal boutons contain round vesicles and apparently synapse only on dendrites.

In several marsupial and placental mammals (opposum: Mendez-Otero et al., '80; tree shrew: Harting et al., '73; cat: Graybiel, '78; Sherk, '79; monkey: Harting et al., '80), the parabigeminal nucleus has a reciprocal topographic connection with the ipsilateral superior colliculus. The main difference between mammals and nonmammals is that the ipsilateral parabigeminal projection avoids terminating in the rostralmost portion of the colliculus where ipsilateral visual fields are represented (except in primates). As in nonmammals, the ipsilateral isthmic afferents terminate extensively throughout the superficial retinal recipient zone and less densely below it (in the intermediate gray) (Graybiel, '79). Rodents are apparently unique in that ipsilaterally projecting parabigeminal neurons are separated into noncontiguous dorsal and ventral cell groups by an intermediate group of contralaterally projecting cells (Watanabe and Kawana, '79; Linden and Perry, '83; Künzle and Schnyder, '84). In other mammals, contralaterally projecting cells do not appear to be segregated.

**The rostral nontopographic nucleus isthmi.** The evidence for a nucleus similar to the rostral magnocellular nucleus isthmi (Imr) of turtles across the vertebrates is less clear-cut, but suggestive data are available for a number of classes. In turtles, Imr receives a nontopographic tectal projection and then projects nontopographically to both Imc and the tectum via bifurcating axons. The very large synaptic boutons given off by Imr axons are rigorously confined to Imc and to the central and periventricular layers of the tectum.

In bony fish, a tectal-receiving nucleus—the nucleus pretectalis—projects strongly to the topographic nucleus isthmi (Ito et al., '81; Sakamoto et al., '81). Nucleus pretectalis terminal boutons in nucleus isthmi are very large and contain flat vesicles (Ito et al., '82). Like turtle Imr, nucleus pretectalis also projects to the tectum (Grover and Sharma, '81).

In the frogs *Rana* and *Acris*, Udin ('87) recently demonstrated a projection to both the contralateral and ipsilateral nucleus isthmi from a scattered group of large cells—the anterodorsal nucleus—located in the mesencephalic tegmentum just rostral to nucleus isthmi. This region receives a tectal input (Masino and Grobstein, '85) and projects as

well to the tectum (Wilczynski and Northcutt, '77). The tegmento-isthmic projection seems rather nontopographic at the single axon level (for example, Fig. 1A in Udin, '87). Its bilateral distribution may be related to the bilateral projection of the medulla of frog nucleus isthmi.

In snakes, nucleus isthmi contains a mixture of small and large neurons, both of which are labeled by ipsilateral tectal injections (Dacey and Ulinski, '86b). Nucleus isthmi injections, in turn, label thin and thick axons in the ipsilateral tectum. The spatially restricted terminal arbors of the thin axons were already mentioned. The thick axons, by contrast, each give rise to a widely spaced series of vertical collaterals that nontopographically innervate the superficial gray layers and especially, the stratum zonale. This contrasts with the deeper layer targets of turtle Imr. Snake nucleus isthmi thus combines features of turtle Imc and Imr.

In lizards, there is a distinct nucleus rostral to the topographic nucleus isthmi that closely resembles turtle Imr in location, morphology, and connections (it receives tectal afferents and projects back to the tectum and to the topographic nucleus) (Wang et al., '83). The topography (if any) of these projections is unknown.

In birds, the magnocellular nucleus isthmi is the probable homologue of the turtle Imr. The avian nucleus receives a nontopographic tectal input via the tectopontine pathway (Hunt and Künzle, '76; Hunt and Brecha, '84) and may project heavily to the topographic nucleus isthmi, Ipc, since injections encroaching on the magnocellular nucleus result in "heavy fibrous labeling" of Ipc (Hunt et al., '77). Antibodies to glutamic acid decarboxylase (GAD) densely stain the somata of magnocellular nucleus isthmi neurons but not Ipc neurons; Ipc is instead filled with large-caliber GAD-stained axon terminals (personal observation, material courtesy Catherine Carr) probably arising from neurons in the magnocellular nucleus. The magnocellular nucleus also projects to the deep layers of the tectum (Hunt and Brecha, '84). Reubi and Cuenod ('76) showed that Ipc stimulation causes GABA release in the pigeon tectum; this may have resulted from the antidromic activation of magnocellular nucleus isthmi axons in Ipc that also project to the tectum. (Abbreviations are confusing here because the avian "magnocellular nucleus isthmi" is usually written as "Imc" while in turtles, "Imc" stands for *caudal* magnocellular nucleus isthmi, the equivalent of avian Ipc.)

In mammals, there are several tectal-recipient cell groups just medial and rostral to the parabigeminal nucleus that project back to the tectum (Graybiel, '78; Künzle and Schnyder, '84). Cells in this region also project to the parabigeminal nucleus (Edwards, '75; Sherk, '79) and may constitute a mammalian counterpart to Imr, though none of the cell groups in mammals are as architectonically distinct as turtle Imr or bird magnocellular nucleus isthmi. Roldan et al. ('83) have reported, in addition, a light, nontopographic projection to the tectum originating from *within* the parabigeminal nucleus, which recalls the situation in snakes.

### Functional implications

A key feature of the circuitry interconnecting Imr, Imc, and the tectum is that topographic and nontopographic visual information is superimposed. Although the nontopographic Imr projection essentially ignores the retinotopic organization of Imc and the tectum, it is strictly confined to these two intimately related structures. Taken together

Fig. 14. Transverse view of a rostral magnocellular nucleus isthmi (Imr) neuron. This cell was labeled by a small tectal injection (see inset). The dendrites (stippled) extend rostrally and caudally and therefore appear quite foreshortened in this transverse reconstruction. The robust, complexly branched axon (origin at open arrow) has three main parts. First, it gives off several local collaterals within Imr that support about 200 large boutons. Second, it sends two main myelinated trunks to the tectum; the thinner branch innervates the caudal face of the tectum while the thicker terminates in the middle and rostral tectum. A portion of the tectal course of the thick trunk (through which the cell was filled) is reconstructed in Figure 15. Finally, the neuron gives off three ventrally and caudally directed trunks that emit large boutons at several different dorsoventral and mediolateral levels within the *caudal* magnocellular nucleus isthmi (Imc, not shown). The inset shows the location of the neuron.

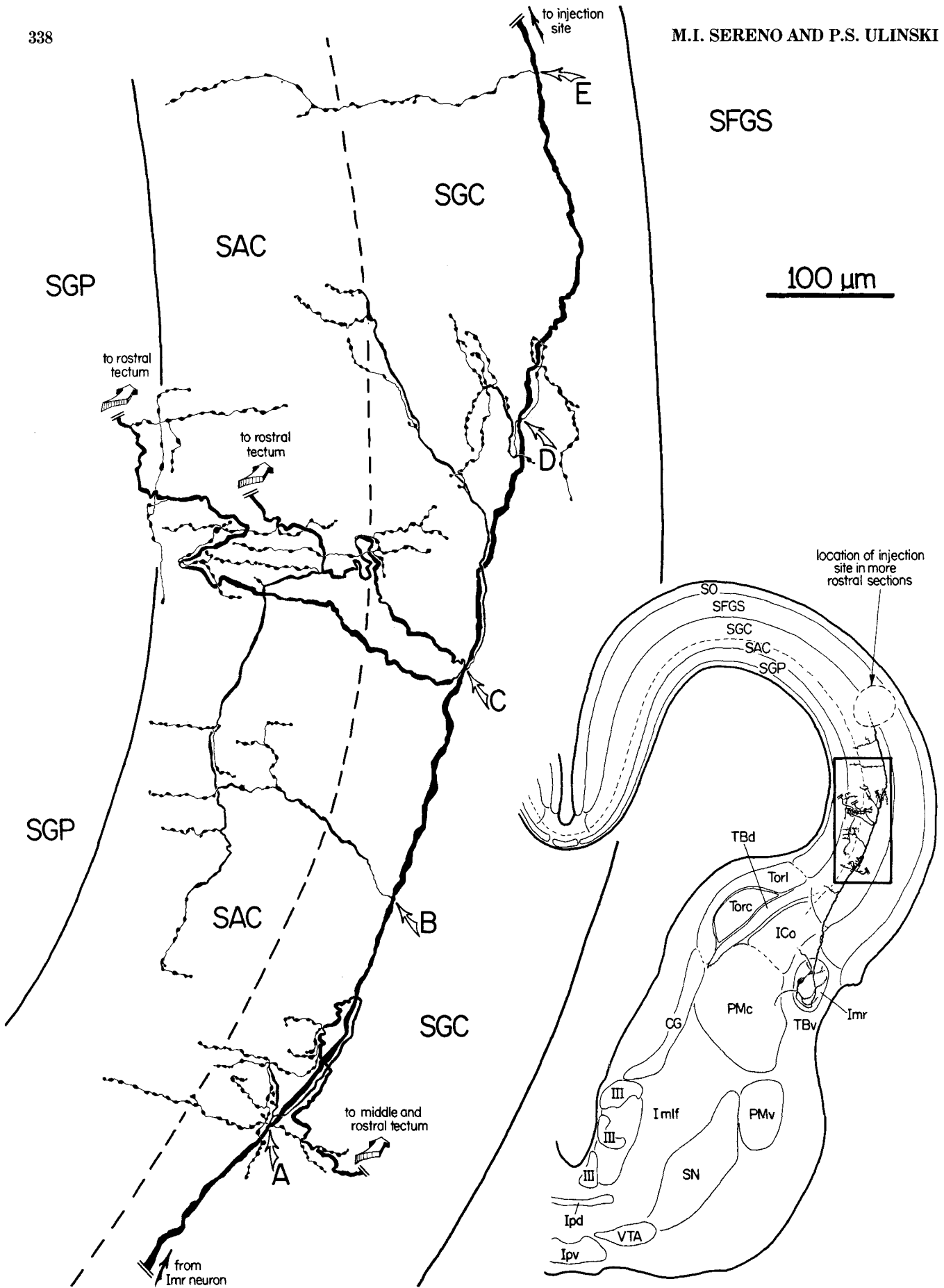


Figure 15

with behavioral, physiological, and histochemical data, the present results suggest several testable hypotheses about the function of these two ipsilateral loops.

**Spatial selective attention.** Ingle ('75) demonstrated in frogs that when a wormlike stimulus is moved briefly enough to avoid eliciting orienting and snapping responses, the stimulated region of the visual field becomes sensitized for several seconds so that a second, similarly brief stimulus, at the same location can often release prey-catching. Recordings made in the superficial laminae of the tectum of immobilized frogs reveal "attention units" with small receptive fields that give a slow, steady discharge for 3-6 seconds after a 1- or 2-second delay. These units are abolished by knife cuts at the caudolateral edge of the tectum that interrupt the ipsilateral but not the contralateral isthmotectal pathway (Ingle, personal communication), suggesting that they are (or depend strongly on input from) nucleus isthmi terminals. Interestingly, a similar pattern of delayed, prolonged excitation has been recorded in the nucleus isthmi of a lizard (Wang et al., '83) and a teleost fish (Williams et al., '83).

These results suggests that the topographically organized ipsilateral isthmotectal pathway may provide punctate positive feedback to the tectum, with nucleus isthmi acting as a sort of scratchpad on which interesting target locations can be temporarily written. Subtotal lesions of nucleus isthmi in frogs result in a permanent contralateral visual scotoma inside which prey and threatening stimuli are ineffective in eliciting snapping and avoidance responses (Caine and Gruberg, '85). Outside the scotoma, prey-catching and threat-avoidance are normal. The scotoma appears very similar to that produced by tectal lesions (Ingle, '73; see also parallels between the effects of tectal and isthmic lesions in pigeons—Hodos and Karten, '74; Jarvis, '74), suggesting that isthmic feedback may not only highlight a

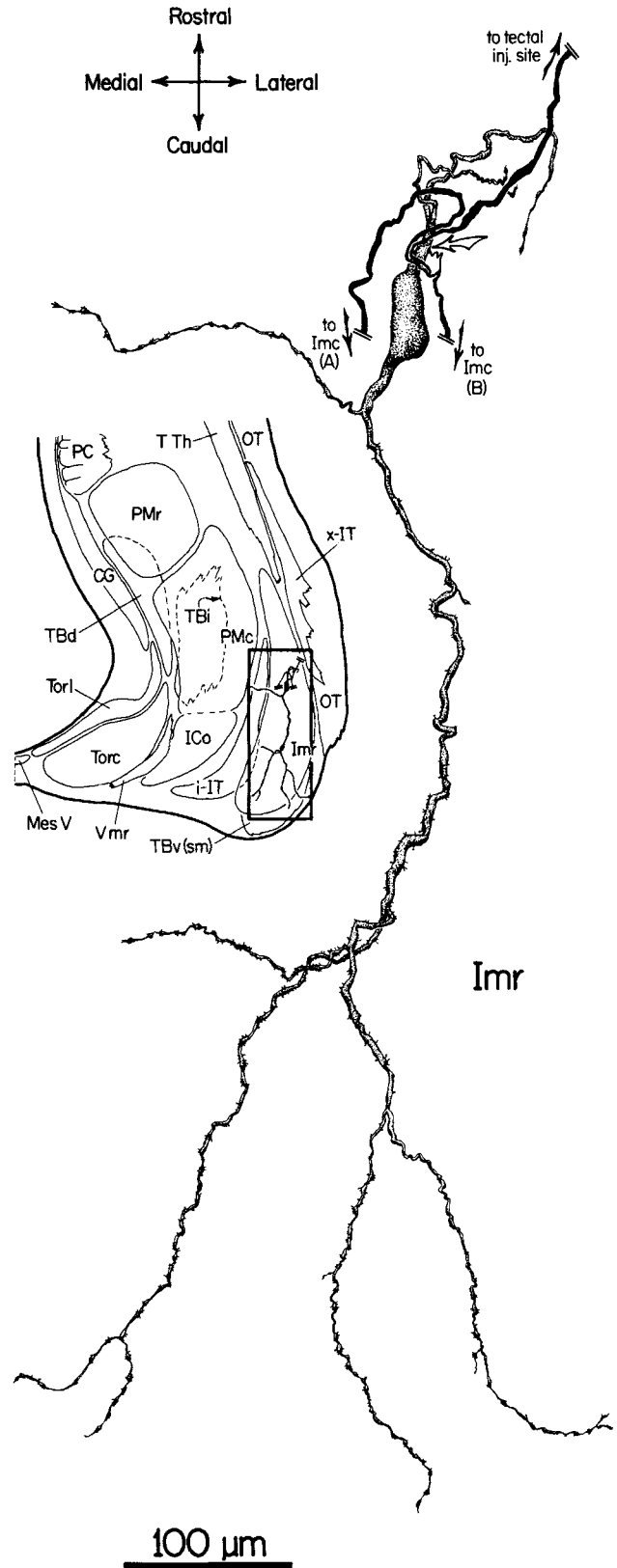


Fig. 15. Continuation of the thicker tectal branch of the rostral magnocellular nucleus isthmi (Imr) neuron shown in Figure 14. The main myelinated trunk courses through the stratum griseum centrale (SGC) emitting thin, vertically oriented strings of large boutons at about 200 μm intervals (branch points A-E). For comparison, an entire Imc terminal arbor would fit between just two of these collaterals. In addition to the thin branches, thicker myelinated collaterals arise at some branch points (one at A and two at C) and course rostrally (3-D arrows) through the SGC and the stratum album centrale (SAC) to reach the middle and far rostral tectum, emitting vertically oriented strings of boutons at regular intervals the whole way (not illustrated). A single Imr axon, thus, sparsely innervates a large percentage of the tectal hemisphere. The inset shows the location of the high-power view.

Fig. 16. Horizontal view of a rostral magnocellular nucleus isthmi (Imr) neuron. This cell was labeled by a small tectal injection. Its large, rostrocaudally elongated, sparsely branched dendritic field is typical for Imr neurons, but its soma is more eccentrically placed than most. The robust (6 μm diameter) axon (origin at open arrow) trifurcated almost immediately into a thick tectal trunk and two other myelinated trunks, labeled A and B, that descend to caudal magnocellular nucleus isthmi (Imc). The terminal arborization in Imc arising from trunks A and B is illustrated in Figure 17 (branch B itself bifurcates on the way to Imc). This neuron apparently lacked local collaterals in Imr, which were usually found on such neurons. The inset shows the location of the high-power view.

Figure 16

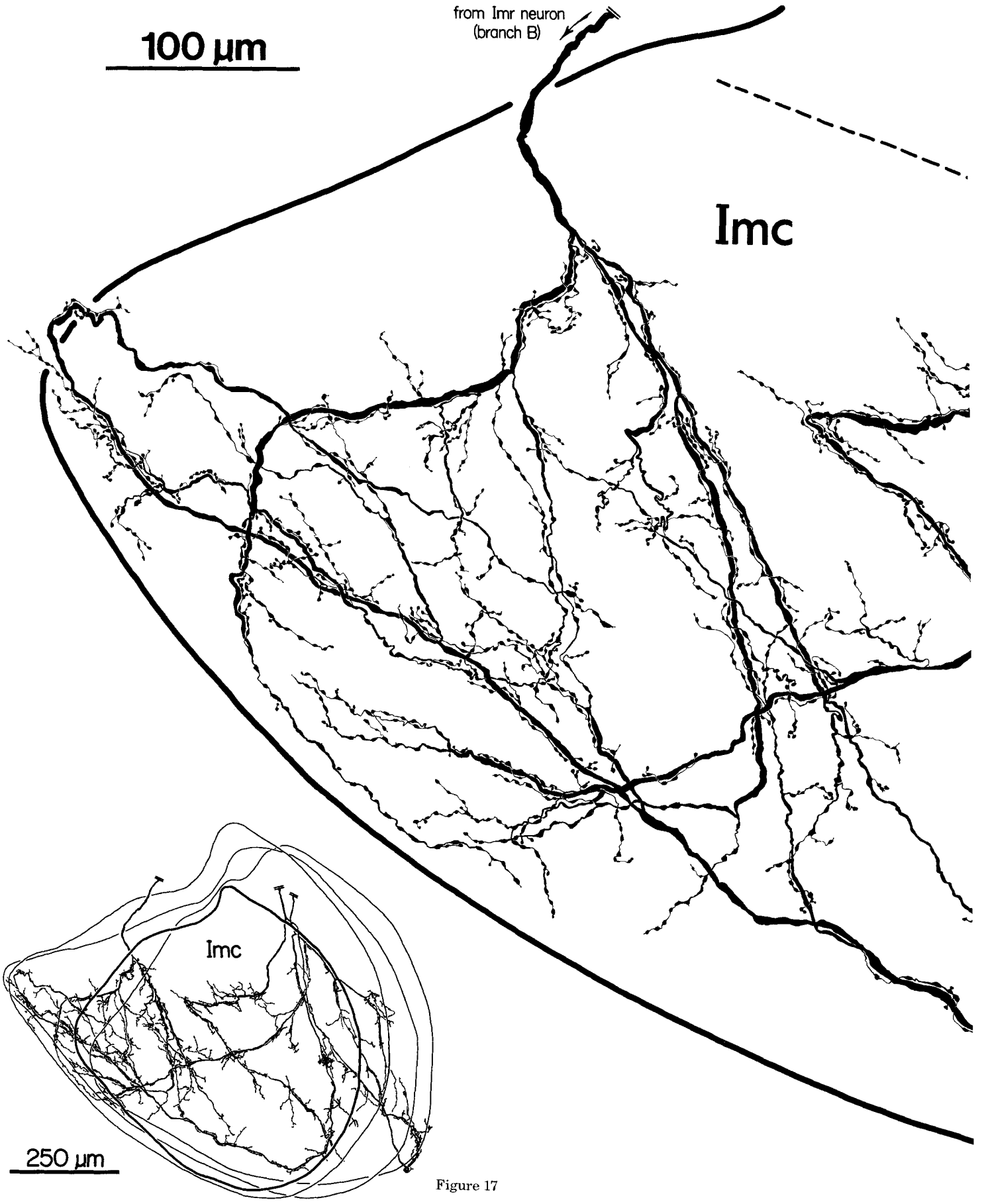
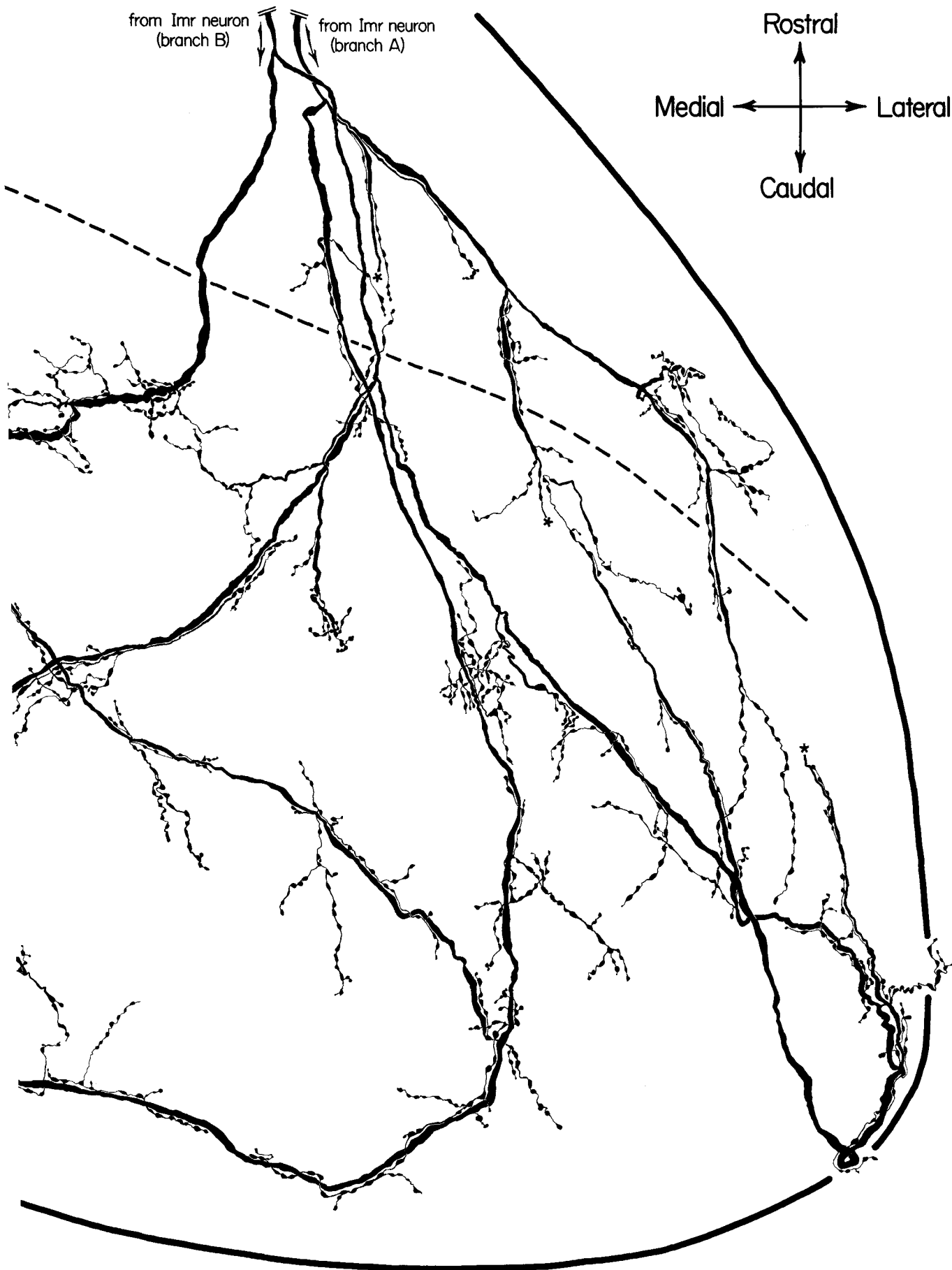


Figure 17



from Imr neuron  
(branch B)

from Imr neuron  
(branch A)

Rostral

Medial ← → Lateral

Caudal

certain visual field location but may be involved in initiating the tectoreticular-mediated orienting response toward it.

The role of the ipsilateral isthomotectal projection in spatial selective attention could be investigated by locally stimulating the topographic nucleus isthmi and determining the effects on tectal output cells and orienting movements and by recording from that nucleus during awake orienting. In vitro slice experiments would help to determine if the delayed, prolonged excitation attributed to ipsilaterally projecting nucleus isthmi neurons is generated intrinsically or by positive feedback. Tectally mediated visuomotor responses are influenced by other cell groups (for example, pretectum) and it would be interesting to compare nucleus-isthmi-mediated effects to those mediated by other structures.

**Local-global interactions.** Frost et al. ('81, '84) showed that direction-selective neurons in all but the most superficial layers of the pigeon tectum typically have large stimulus-specific inhibitory surrounds extending far beyond the edges of their excitatory receptive fields and sometimes including the entire visual field. Moving a random dot pattern through the surround completely suppresses the response to an optimal receptive field stimulus (moving bar or random dot patch) if the surround moves "in phase" with it, but enhances the response if the surround moves in the opposite direction. (By themselves, the different surround stimuli produce no effect as long as they remain outside the excitatory receptive field.) In addition, moving the surround in a given direction changes the best direction of the receptive field center to the opposing direction for many of these cells (Frost and Nakayama, '83). This effect is so strong that the peak in the direction tuning curve of the receptive field center can be shifted 180°C. Stimulus-specific inhibitory surrounds have also been observed in the tectum of

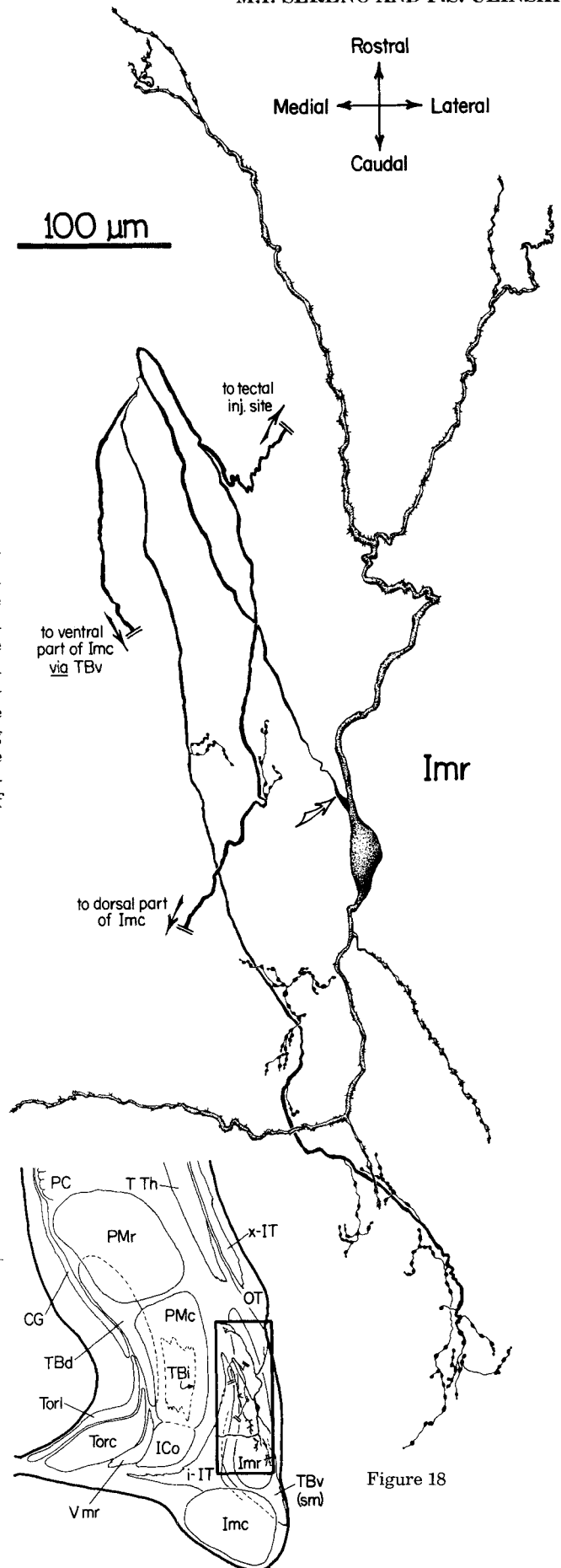


Fig. 17. (See the two previous pages for figure.) Termination of rostral magnocellular nucleus isthmi (Imr) axon (branches A and B from Imr cell shown in Fig. 16) in caudal magnocellular nucleus isthmi (Imc). This Imr cell terminal arbor was labeled by a small tectal injection (via the axon's tectal branch) and reconstructed from seven horizontal sections. Three thick, myelinated trunks (one is branch A while two are from branch B, which bifurcated on its way to Imc) enter Imc from the front. These each subdivide into several myelinated branches that begin wandering to and fro, emitting strings of large (2–3.5 μm) boutons. The boutons (1,840 total) are distributed across many mediolateral and dorsoventral levels of the Imc cell plate but remain strictly confined to the nucleus. Small, overlapping clusters of tecto-isthmic terminals and Imc neurons also labeled by the tectal injection were located in the lateral third of the nucleus, emphasizing the nontopographic nature of this terminal arbor. Three asterisks indicate where small trunks were lost before they ended. The inset shows the location of the terminal arbor and the outlines of Imc in some of the sections used in the reconstruction.

Fig. 18. Horizontal view of a rostral magnocellular nucleus isthmi (Imr) neuron. This cell was labeled by a small tectal injection. The large, rostrocaudally elongated dendritic field is seen almost *en face* in this reconstruction. As with the Imr neuron in Figure 14, the robust axon of this neuron (origin at open arrow) emits a few local collaterals in Imr (supporting about 150 boutons), a thick tectal branch that innervates a large portion of the tectum, and several branches to different parts of the map in caudal magnocellular nucleus isthmi (Imc). The dendrites (stippled) of this and other Imr neurons are covered with fine spicules like those seen on dorsal and intermediate tectobulbar neurons (Sereno and Ulinski, '85). The inset shows the location of the neuron.

Figure 18

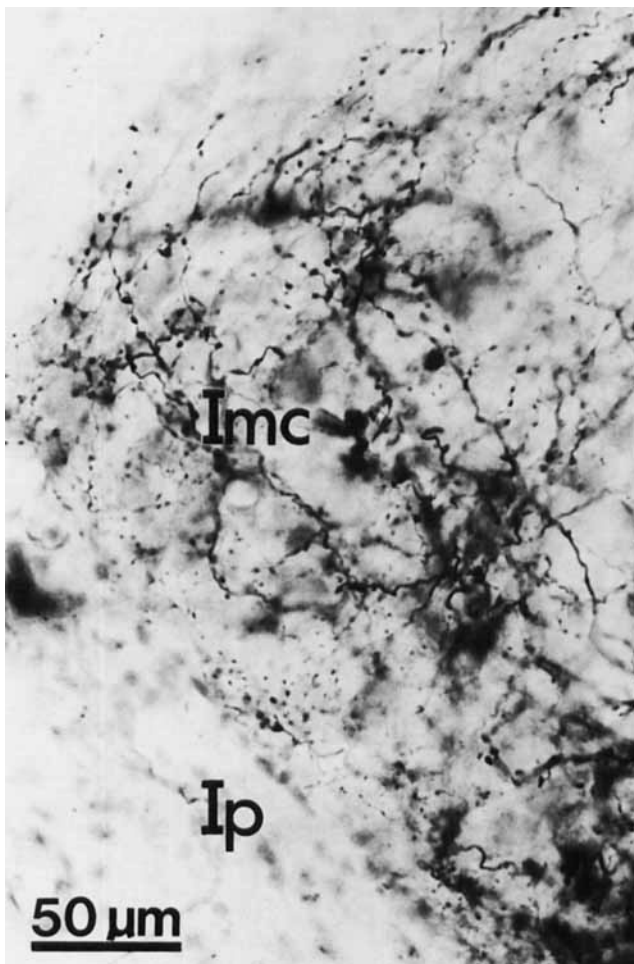


Fig. 19. High-magnification view (upper left-hand corner) of the nontopographic background labeling of Imc shown in the low-power photomicrograph in Figure 1B. The axon terminals here were labeled by a large tectal injection. They appear not to be tectal afferents, but rather, branched afferents from Imr that innervate both Imc and the tectum (see text and Figs. 14–18). The robust (2–3.5  $\mu\text{m}$  diameter) boutons are distributed quite uniformly throughout the entire volume of Imc in marked contrast to the restricted band of tectoisthmic terminals and Imc cells also labeled by the injection. The nontopographic label is, however, rigorously confined to Imc, effectively outlining the nucleus.

frogs (Burghagen and Ewert, '83) and in the superior colliculus of cats (Sterling and Wickelgren, '69).

These mechanisms could mediate the discrimination of object motion from self-induced motion (Ewert, '84; Allman et al., '85). To find out whether the nontopographic nucleus isthmi is involved in generating these effects, one could record from a tectal cell with a surround and then inactivate the nontopographic nucleus isthmi with lidocaine to see if the stimulus-specific surround inhibition is made nonselective or abolished. One would also expect to find wide-field direction-selective cells in nontopographic nucleus isthmi and small-field cells with large surrounds in topographic nucleus isthmi.

**Arbitration of competing stimuli.** An alternate function of the nontopographic nucleus isthmi may be to participate closely with topographic nucleus isthmi in the construction of a "winner-take-all" network (Feldman, '82; Koch and Ullman, '85) in the tectum. An obvious problem in generating tectoreticular-mediated orienting responses is that there may be more than one possible interesting new target simultaneously present in the pattern of activity sent to the superficial layers of the tectum by the retina; but only one locus in the deeper-lying motor map (see Sereno and Ulinski, '85, for discussion) must be activated to avoid orienting to the "average" of the stimuli, Koch and Ullman ('85) present two model networks that perform a maximum-finding computation. The two tecto-isthmo-tectal loops described here appear to form a network like their first one.

They set up a "saliency map" (cf. the superficial tectum) that directly drives a "winner-take-all" map (cf. the intermediate and deep tectum); in the latter, the most active locus suppresses all other activated loci while itself being driven to saturation. The update rule for the "winner-take-all" network is: if a unit's input is greater than the average input for the whole map, increase that unit's output in proportion to the difference, while if its input is below average, decrease its output in the same manner. Something similar to this in principle may describe the action of the ipsilateral isthmic nuclei on the motor map in the tectum. The positive feedback loop between the tectum and topographic nucleus isthmi (or the intrinsic properties of topographic nucleus isthmi neurons) could provide a multiplicative or exponential augmentation of activated loci necessary to always give the most active locus the advantage. The nontopographic nucleus isthmi is in a position to calculate the average input to tectoreticular neurons, and its direct and indirect nontopographic outputs to the tectum could uniformly inhibit all tectal loci, eventually suppressing all but the most active locus. The local collaterals of the nontopographic nucleus isthmi neurons could control the gain of the inhibition. The main difference from Koch and Ullman's presentation is that excitatory and inhibitory influences are carried by separate pathways that differ in more than their sign of action.

Inactivation of nontopographic nucleus isthmi should in this case result in disinhibition of tectal and topographic nucleus isthmi neurons to receptive field stimuli along with a loss of nonspecific surround inhibition (direction-selective inhibition, for instance, might remain if it is mediated through pretectal or intrinsic tectal circuits). In addition, this scenario predicts no direction-selective neurons in nontopographic nucleus isthmi. At the behavioral level, ibotenic acid lesions in that nucleus should produce deficits in orienting when several salient stimuli are present.

#### ACKNOWLEDGMENTS

This work was supported by PHS grant NS 12518 and an NSF predoctoral fellowship.

#### LITERATURE CITED

- Adams, J.C. (1977) Technical considerations on the use of horseradish peroxidase as a neuronal marker. *Neuroscience* 2:141–145.
- Allman, J., F. Miezin, and E. McGuinness (1985) Stimulus specific responses from far beyond the classical receptive field: Neurophysiological mechanisms for local-global comparisons in visual neurons. *Annu. Rev. Neurosci.* 8:407–429.
- Brauth, S.E., A. Reiner, C.A. Kitt, and H.J. Karten (1983) The substance-P-containing striatoreticular path in reptiles: An immunohistochemical study. *J. Comp. Neurol.* 219:305–327.

# Imc neuron

# Imr neuron

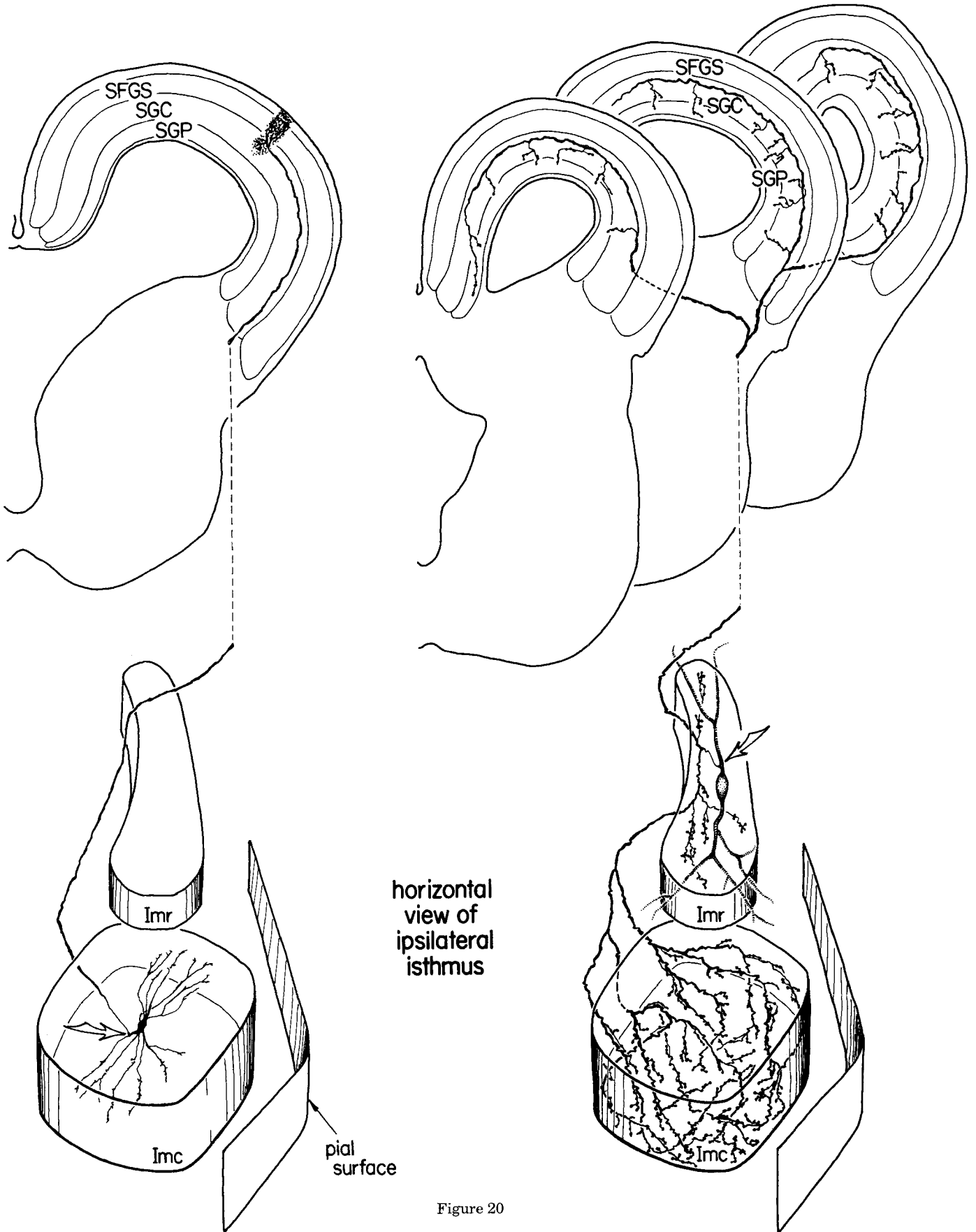


Figure 20

- Burghagen, H., and J.-P. Ewert (1983) Influence of the background for discriminating object motion from self-induced motion in toads *Bufo bufo* (L.). *J. Comp. Physiol.* 152:241-249.
- Caine, H.S., and E.R. Gruberg (1985) Ablation of nucleus isthmi leads to loss of specific visually elicited behaviors in the frog *Rana pipiens*. *Neurosci. Lett.* 54:307-312.
- Cajal, S. Ramon y (1899) Adiciones a nuestros trabajos sobre los centros opticos de las aves. *Rev. Trimest. Microgr.* 4:77-86.
- Cruce, W.L.R., and R. Nieuwenhuys (1974) The cell masses in the brainstem of the turtle *Testudo hermanni*. *J. Comp. Neurol.* 156:277-306.
- Dacey, D.M., and P.S. Ulinski (1986a) The optic tectum of the eastern garter snake, *Thamnophis sirtalis*: II. Morphology of efferent cells. *J. Comp. Neurol.* 245:198-327.
- Dacey, D.M., and P.S. Ulinski (1986b) The optic tectum of the eastern garter snake, *Thamnophis sirtalis*: V. Morphology of brainstem afferents and general discussion. *J. Comp. Neurol.* 245:423-453.
- Desan, P.H., E.R. Gruberg, and F. Eckenstein (1984) A cholinergic projection from the nucleus isthmi to the optic tectum in turtle and frog. *Proc. Soc. Neurosci.* 10:575 (Abstract).
- Edwards, S.B. (1975) Autoradiographic studies of the projections of the midbrain reticular formation: Descending projection of the nucleus cuneiformis. *J. Comp. Neurol.* 161:341-358.
- Ewert, J.-P. (1984) Tectal mechanisms that underlie prey catching and avoidance behaviors in toads. In H. Vanegas (ed): *Comparative Neurology of the Optic Tectum*. New York: Plenum Press, pp. 247-416.
- Feldman, J.A. (1982) Dynamic connections in neural networks. *Biol. Cybern.* 46:27-39.
- Foster, R.E. and W.C. Hall (1975) The connections and laminar organization of the optic tectum in a reptile (*Iguana iguana*). *J. Comp. Neurol.* 163:397-426.
- Frost, B.J., P. Cavanagh, and B. Morgan (1984) Kinetograms drive deep tectal cells in pigeons. *Proc. Soc. Neurosci.* 10:574 (Abstract).
- Frost, B.J., and K. Nakayama (1983) Single visual neurons code opposing motion independent of direction. *Science* 220:744-745.
- Frost, B.J., P.L. Scilley, and S.C.P. Wong (1981) Moving background patterns reveal double-opponency of directionally specific pigeon tectal neurons. *Exp. Brain Res.* 42:173-185.
- Glasser, S., and D. Ingle (1978) The nucleus isthmi as a relay station in the ipsilateral visual projection to the frog's optic tectum. *Brain Res.* 159:214-218.
- Glenn, L.L., and R.E. Burke (1981) A simple and inexpensive method for 3-dimensional visualization of neurons reconstructed from serial sections. *J. Neurosci. Methods.* 4:127-134.
- Graybiel, A.M. (1978) A satellite system of the superior colliculus: The parabigeminal nucleus and its projection to the superficial collicular layers. *Brain Res.* 145:365-374.
- Grobstein, P., C. Comer, M. Hollyday, and S.M. Archer (1978) A crossed isthmo-tectal projection and its movement in the ipsilateral visuo-tectal projection. *Brain Res.* 156:117-123.
- Grobstein, P., and C. Comer (1983) The nucleus isthmi as an intertectal relay for the ipsilateral oculotectal projection in the frog *Rana pipiens*. *J. Comp. Neurol.* 217:54-74.
- Grover, B.G., and S.C. Sharma (1981) Organization of extrinsic tectal connections in goldfish (*Carassius auratus*). *J. Comp. Neurol.* 196:471-488.
- Gruberg, E.R., and J.Y. Lettvin (1980) Anatomy and physiology of a binocular system in the frog, *Rana pipiens*. *Brain Res.* 192:313-325.
- Gruberg, E.R., and S.B. Udin (1978) Topographic projections between the nucleus isthmi and the tectum of the frog, *Rana pipiens*. *J. Comp. Neurol.* 179:487-500.
- Harting, J.K., W.C. Hall, I.T. Diamond, and G.F. Martin (1973) Anterograde degeneration study of the superior colliculus in *Tupaia glis*: Evidence for a subdivision between superficial and deep layers. *J. Comp. Neurol.* 148:361-386.
- Harting, J.K., M.F. Huerta, A.J. Frankfurter, N.L. Strominger, and G.L. Royce (1980) Ascending pathways from the monkey superior colliculus: An autoradiographic analysis. *J. Comp. Neurol.* 192:852-882.
- Henley, J.M., J.M. Lindstrom, and R.E. Oswald (1986) Acetylcholine receptor synthesis in retina and transport to optic tectum in goldfish. *Science* 232:1627-1629.
- Hodos, W., and H.J. Karten (1974) Visual intensity and pattern discrimination deficits after lesions of the optic lobe in pigeons. *Brain Behav. Evol.* 9:165-194.
- Hunt, S.P., and N. Brecha (1984) The avian optic tectum: A synthesis of morphology and biochemistry. In H. Vanegas (ed): *Comparative Neurology of the Optic Tectum*. New York: Plenum Press, pp. 619-648.
- Hunt, S.P., and H. Künzle (1976) Observations on the projections and intrinsic organization of the pigeon optic tectum: An autoradiographic study based on anterograde and retrograde, axonal and dendritic flow. *J. Comp. Neurol.* 170:153-172.
- Hunt, S.P., P. Streit, H. Künzle, and M. Cuenod (1977) Characterization of the pigeon isthmotectal pathway by selective uptake and retrograde movement of radioactive compounds and by Golgi-like horseradish peroxidase labelling. *Brain Res.* 129:197-212.
- Ingle, D. (1973) Two visual systems in the frog. *Science* 181:1053-1055.
- Ingle, D. (1975) Selective visual attention in frogs. *Science* 188:1033-1035.
- Ito, H., N. Sakamoto, and K. Takatsuji (1982) Cytoarchitecture, fiber connections and ultrastructure of nucleus isthmi in a teleost (*Navodon modestus*) with a special reference to degenerating isthmic afferents from optic tectum and nucleus pretectalis. *J. Comp. Neurol.* 205:299-311.
- Ito, H., H. Tanaka, N. Sakamoto, and Y. Morita (1981) Isthmic afferent neurons identified by retrograde HRP method in a teleost, *Navodon modestus*. *Brain Res.* 207:163-169.
- Jarvis, C.D. (1974) Visual discrimination and spatial localization deficits after lesions of the tectofugal pathways in pigeons. *Brain Behav. Evol.* 9:195-228.
- Koch, C., and S. Ullman (1985) Shifts in selective attention: Toward the underlying neural circuitry. *Hum. Neurobiol.* 4:219-227.
- Künzle, H., and H. Schnyder (1984) The isthmus-tegmentum complex in the turtle and rat: A comparative analysis of its interconnections with the optic tectum. *Exp. Brain Res.* 56:509-522.
- Lazar, G. (1984) Structure and connections of the frog tectum. In H. Vanegas (ed): *Comparative Neurology of the Optic Tectum*. New York: Plenum Press, pp. 185-210.
- Linden, R., and V.H. Perry (1983) Retrograde and anterograde-transneuronal degeneration in the parabigeminal nucleus following tectal lesions in developing rat. *J. Comp. Neurol.* 218:270-281.
- Masino, T., and P. Grobstein (1985) The organization of tectal projections to the ventral midbrain in *Rana pipiens*. *Proc. Soc. Neurosci.* 11:289 (Abstract).
- Mendez-Otero, R., C.E. Rocha-Miranda, and V.H. Perry (1980) The organization of the parabigemino-tectal projections in the opossum. *Brain Res.* 198:183-189.
- Reubi, J.-C., and M. Cuenod (1976) Release of exogenous glycine in the pigeon optic tectum during stimulation of a midbrain nucleus. *Brain Res.* 112:346-361.
- Roldan, M., F. Reinoso-Suarez, and A. Tortelly (1983) Parabigeminal projections to the superior colliculus. *Brain Res.* 280:1-13.
- Sakamoto, N., H. Ito, and S. Ueda (1981) Topographic projection between the nucleus isthmi and the optic tectum in a teleost, *Navodon modestus*. *Brain Res.* 224:225-234.
- Sereno, M.I. (1985) Tectoreticular pathways in the turtle, *Pseudemys scripta*. I. Morphology of tectoreticular axons. *J. Comp. Neurol.* 233:48-90.
- Sereno, M.I., and P.S. Ulinski (1985) Tectoreticular pathways in the turtle, *Pseudemys scripta*. II. Morphology of tectoreticular cells. *J. Comp. Neurol.* 233:91-114.
- Sherk, H. (1979) Connections and visual-field mapping in cat's tectoparabigeminal circuit. *J. Neurophysiol.* 42:1656-1668.
- Sterling, P., and B.G. Wickelgren (1969) Visual receptive fields in the superior colliculus of the cat. *J. Neurophysiol.* 32:1-15.
- ten Donkelaar, H.J., and R. Nieuwenhuys (1979) The brain stem. In C. Gans, R.G. Northcutt, and P.S. Ulinski (eds): *Biology of the Reptilia*, Vol. 10. Neurology B. London: Academic Press, pp. 133-200.
- Udin, S.B. (1986) A projection from the mesencephalic tegmentum to the nucleus isthmi in the frogs, *Rana pipiens* and *Acris crepitans*. *Neuroscience* (in press).

Fig. 20. Schematic diagram of the typical axonal and dendritic morphology of single caudal magnocellular nucleus isthmi (Imc) and rostral magnocellular nucleus isthmi (Imr) neurons, drawn to the same scale. The two isthmic nuclei have been enlarged relative to the tectum for clarity. The restricted dendritic and axonal arbors of Imc neurons contrast with the strikingly nontopographic projection of the larger Imr neurons not only to the tectum but also to Imc.

- Wang, R., J.L. Kubie, and M. Halpern (1977) Brevital Sodium: An effective anesthetic agent for performing surgery on small reptiles. *Copeia* 1977:739-743.
- Wang, S.-R., K. Yan, Y.-T. Wang, S.-J. Jiang, and X.-S. Wang (1983) Neuroanatomy and electrophysiology of the lacertilian nucleus isthmi. *Brain Res.* 275:355-360.
- Watanabe, K., and E. Kawana (1979) Efferent projections of the parabrachial nucleus in rats: A horseradish peroxidase (HRP) study. *Brain Res.* 168:1-11.
- Wilczynski, W., and R.G. Northcutt (1977) Afferents to the optic tectum of the leopard frog: An HRP study. *J. Comp. Neurol.* 173:219-230.
- Williams, B., N. Hernandez, and H. Vanegas (1983) Electrophysiological analysis of the telostean nucleus isthmi and its relationship with the optic tectum. *J. Comp. Physiol. A* 152:545-554.
- Vanegas, H., S.O.E. Ebbesson, and M. Laufer (1984) Morphological aspects of the telostean optic tectum. In H. Vanegas (ed): *Comparative Neurology of the Optic Tectum*. New York: Plenum Press, pp. 93-120.